Real-time techniques and topological data analysis for non-perturbative phenomena in QFT

Daniel Spitz (University of Heidelberg)

Efficient simulations on GPU hardware, ETH Zurich

October 26th, 2022

isoQuant SFB1225

STRUCTURES CLUSTER OF EXCELLENCE

UNIVERSITÄT HEIDELBERG ZUKUNFT SEIT 1386

Content

1. Lattice improved Hamiltonians for classical-statistical simulations
2. Non-thermal fixed points in persistent homology
3. Confinement in persistent homology
4. Conclusions & outlook

Content

1. Lattice improved Hamiltonians for classical-statistical simulations

2. Non-thermal fixed points in persistent homology

3. Confinement in persistent homology

4. Conclusions & outlook

Classical-statistical real-time simulations for gauge theories

Classical-statistical real-time simulations for gauge theories

Nonequilibrium phenomena require QFT formulated on a **Keldysh contour**:

[Kadanoff & Baym, 1962; Keldysh, 1965; Berges, 2004; Calzetta & Hu, 2008]

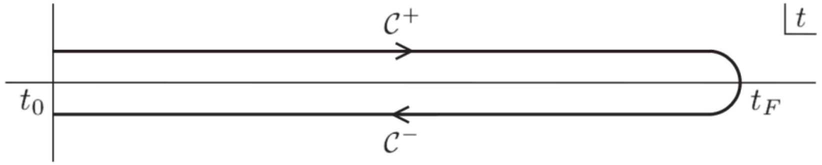

Classical-statistical real-time simulations for gauge theories

Nonequilibrium phenomena require QFT formulated on a **Keldysh contour**:

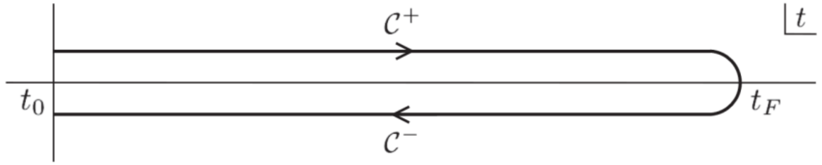

[Kadanoff & Baym, 1962; Keldysh, 1965; Berges, 2004; Calzetta & Hu, 2008]

Decompose gauge fields on $\mathcal{C}$ into classical and quantum fields: $A_\mu(x) = \bar{A}_\mu(\mathrm{pr}_t(x)) + \frac{1}{2}\tilde{A}_\mu(\mathrm{pr}_t(x))\mathrm{sgn}_\mathcal{C}(x^0)$

Classical-statistical real-time simulations for gauge theories

Nonequilibrium phenomena require QFT formulated on a **Keldysh contour**:

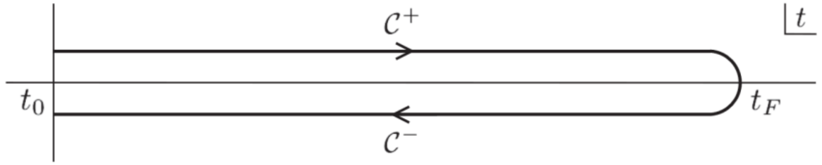

[Kadanoff & Baym, 1962; Keldysh, 1965;
Berges, 2004; Calzetta & Hu, 2008]

Decompose gauge fields on $\mathcal{C}$ into classical and quantum fields: $A_\mu(x) = \bar{A}_\mu(\mathrm{pr}_t(x)) + \frac{1}{2}\tilde{A}_\mu(\mathrm{pr}_t(x))\mathrm{sgn}_{\mathcal{C}}(x^0)$

Keep in action on $\mathcal{C}$ only terms up to quadratic order in $\tilde{A}_\mu$, then integrate out $\tilde{A}_\mu$ in path integrals.
Then:

[Hebenstreit *et al.*, 2013; Kasper *et al.*, 2014]

$$\langle \mathcal{O}[\bar{A}] \rangle = \int D\bar{A}_{t_0}\, D\bar{E}_{t_0}\, W[\bar{A}_{t_0}, \bar{E}_{t_0}]\, \mathcal{O}_{\mathrm{cl}}[\bar{A}_{t_0}, \bar{E}_{t_0}],$$

$$\mathcal{O}_{\mathrm{cl}}[\bar{A}_{t_0}, \bar{E}_{t_0}] = \int D\bar{A}\, \mathcal{O}[\bar{A}]\, \delta(\bar{A} - \bar{A}_{\mathrm{cl}}[\bar{A}_{t_0}, \bar{E}_{t_0}])$$

with $\bar{A}_{\mathrm{cl}}[\bar{A}_{t_0}, \bar{E}_{t_0}]$ solution of **classical eom.** for gauge theory with given ini. conditions.

Classical-statistical real-time simulations for gauge theories

Nonequilibrium phenomena require QFT formulated on a **Keldysh contour**:

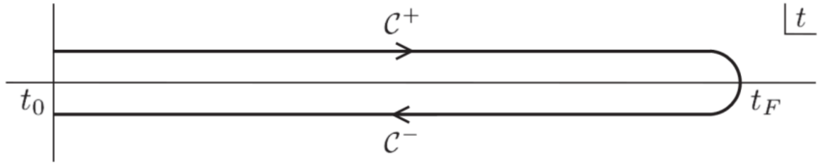

[Kadanoff & Baym, 1962; Keldysh, 1965; Berges, 2004; Calzetta & Hu, 2008]

Decompose gauge fields on $\mathcal{C}$ into classical and quantum fields: $A_\mu(x) = \bar{A}_\mu(\mathrm{pr}_t(x)) + \frac{1}{2}\tilde{A}_\mu(\mathrm{pr}_t(x))\mathrm{sgn}_{\mathcal{C}}(x^0)$

Keep in action on $\mathcal{C}$ only terms up to quadratic order in $\tilde{A}_\mu$, then integrate out $\tilde{A}_\mu$ in path integrals.
Then:

[Hebenstreit *et al.*, 2013; Kasper *et al.*, 2014]

$$\langle \mathcal{O}[\bar{A}] \rangle = \int D\bar{A}_{t_0}\, D\bar{E}_{t_0}\, W[\bar{A}_{t_0}, \bar{E}_{t_0}]\, \mathcal{O}_{\mathrm{cl}}[\bar{A}_{t_0}, \bar{E}_{t_0}],$$

$$\mathcal{O}_{\mathrm{cl}}[\bar{A}_{t_0}, \bar{E}_{t_0}] = \int D\bar{A}\, \mathcal{O}[\bar{A}]\, \delta(\bar{A} - \bar{A}_{\mathrm{cl}}[\bar{A}_{t_0}, \bar{E}_{t_0}])$$

with $\bar{A}_{\mathrm{cl}}[\bar{A}_{t_0}, \bar{E}_{t_0}]$ solution of **classical eom.** for gauge theory with given ini. conditions.

Approximation is **good for small couplings and many gauge bosons.** [Aarts & Berges, 2002; Berges & Gasenzer, 2007]

Lattice improved Hamiltonians for SU(2) theory with fermions

Lattice improved Hamiltonians for SU(2) theory with fermions

SU(2) Hamiltonian including **improved Wilson fermions**:

$$H(t) = H^{(\mathrm{g})}(t) + H^{(\mathrm{f})}(t) \qquad H^{(\mathrm{g})}(t) = a\sum_{n\in\Lambda} \mathrm{tr} E_n^2(t)$$

$$\begin{aligned} H^{(\mathrm{f})}(t) = a\sum_n \psi_n(t)^\dagger \gamma^0 \Bigg[& (m + Kr/a)\psi_n(t) \\ & - \frac{1}{2a}\sum_{k=1}^{K} C_k(i\gamma^1 + kr)U_{n,k}(t)\psi_{n+k}(t) \\ & + \frac{1}{2a}\sum_{k=1}^{K} C_k(i\gamma^1 - kr)U_{n,-k}(t)\psi_{n-k}(t)\Bigg] \end{aligned}$$

[DS & Berges, 2019]

Lattice improved Hamiltonians for SU(2) theory with fermions

SU(2) Hamiltonian including **improved Wilson fermions**:

$$H(t) = H^{(\mathrm{g})}(t) + H^{(\mathrm{f})}(t) \qquad H^{(\mathrm{g})}(t) = a\sum_{n\in\Lambda} \mathrm{tr} E_n^2(t)$$

$$\begin{aligned} H^{(\mathrm{f})}(t) = a\sum_n \psi_n(t)^\dagger \gamma^0 \Big[&(m + Kr/a)\psi_n(t) \\ &- \frac{1}{2a}\sum_{k=1}^{K} C_k(i\gamma^1 + kr)U_{n,k}(t)\psi_{n+k}(t) \\ &+ \frac{1}{2a}\sum_{k=1}^{K} C_k(i\gamma^1 - kr)U_{n,-k}(t)\psi_{n-k}(t)\Big] \end{aligned}$$

[DS & Berges, 2019]

Classical-statistical reweighting: solve Heisenberg eoms. for electric field, link and fermion operators using this Hamiltonian, sample over Gaussian initial conditions.

Lattice improved Hamiltonians for SU(2) theory with fermions

SU(2) Hamiltonian including **improved Wilson fermions**:

$$H(t) = H^{(\mathrm{g})}(t) + H^{(\mathrm{f})}(t) \qquad H^{(\mathrm{g})}(t) = a\sum_{n\in\Lambda} \mathrm{tr} E_n^2(t)$$

$$\begin{aligned} H^{(\mathrm{f})}(t) = a\sum_n \psi_n(t)^\dagger \gamma^0 \Big[&(m + Kr/a)\psi_n(t) \\ &- \frac{1}{2a}\sum_{k=1}^{K} C_k (i\gamma^1 + kr) U_{n,k}(t)\psi_{n+k}(t) \\ &+ \frac{1}{2a}\sum_{k=1}^{K} C_k (i\gamma^1 - kr) U_{n,-k}(t)\psi_{n-k}(t) \Big] \end{aligned}$$

[DS & Berges, 2019]

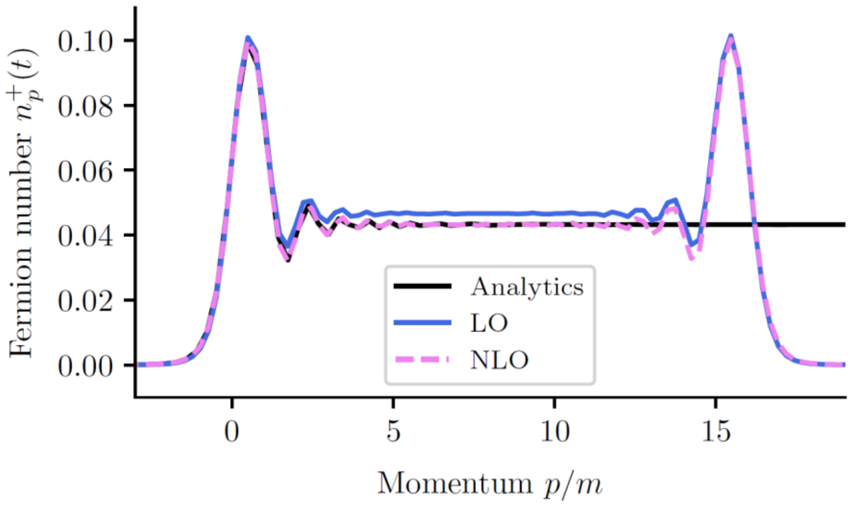

Lattice improvements (LO, NLO and NNLO below) for fermion production from initial chromoelectric field zero mode, compared to analytic one-loop predictions.

Classical-statistical reweighting: solve Heisenberg eoms. for electric field, link and fermion operators using this Hamiltonian, sample over Gaussian initial conditions.

Lattice improved Hamiltonians for SU(2) theory with fermions

SU(2) Hamiltonian including **improved Wilson fermions**:

$$H(t) = H^{(\mathrm{g})}(t) + H^{(\mathrm{f})}(t) \qquad H^{(\mathrm{g})}(t) = a\sum_{n\in\Lambda} \mathrm{tr} E_n^2(t)$$

$$\begin{aligned} H^{(\mathrm{f})}(t) = a\sum_n \psi_n(t)^\dagger \gamma^0 \Big[& (m + Kr/a)\psi_n(t) \\ & - \frac{1}{2a}\sum_{k=1}^{K} C_k (i\gamma^1 + kr) U_{n,k}(t)\psi_{n+k}(t) \\ & + \frac{1}{2a}\sum_{k=1}^{K} C_k (i\gamma^1 - kr) U_{n,-k}(t)\psi_{n-k}(t) \Big] \end{aligned}$$

[DS & Berges, 2019]

Classical-statistical reweighting: solve Heisenberg eoms. for electric field, link and fermion operators using this Hamiltonian, sample over Gaussian initial conditions.

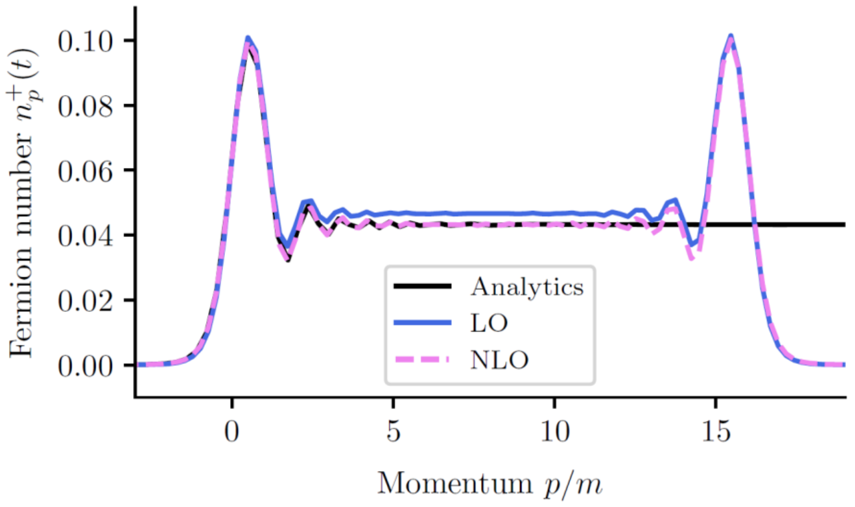

Lattice improvements (LO, NLO and NNLO below) for fermion production from initial chromoelectric field zero mode, compared to analytic one-loop predictions.

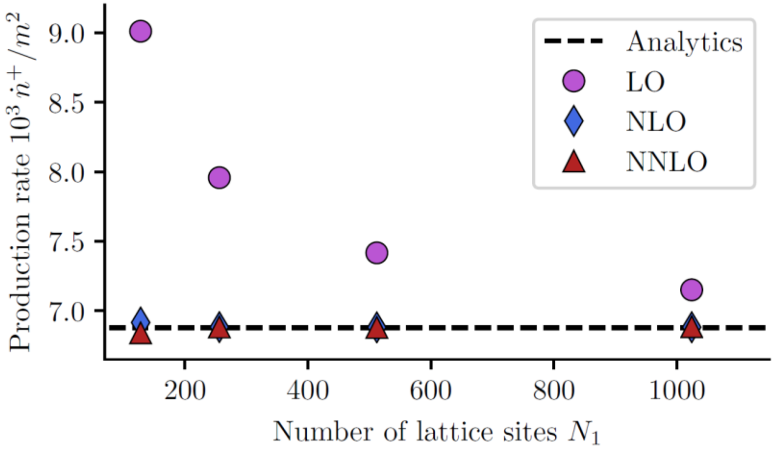

Lattice improved Hamiltonians for SU(2) theory with fermions

SU(2) Hamiltonian including **improved Wilson fermions**:

$$H(t) = H^{(\mathrm{g})}(t) + H^{(\mathrm{f})}(t) \qquad H^{(\mathrm{g})}(t) = a\sum_{n\in\Lambda}\mathrm{tr}E_n^2(t)$$

$$H^{(\mathrm{f})}(t) = a\sum_n \psi_n(t)^\dagger\gamma^0\Big[(m + Kr/a)\psi_n(t) - \frac{1}{2a}\sum_{k=1}^{K} C_k(i\gamma^1 + kr)U_{n,k}(t)\psi_{n+k}(t) + \frac{1}{2a}\sum_{k=1}^{K} C_k(i\gamma^1 - kr)U_{n,-k}(t)\psi_{n-k}(t)\Big]$$

[DS & Berges, 2019]

Classical-statistical reweighting: solve Heisenberg eoms. for electric field, link and fermion operators using this Hamiltonian, sample over Gaussian initial conditions.

Lattice improvements vastly improve large-volume convergence!

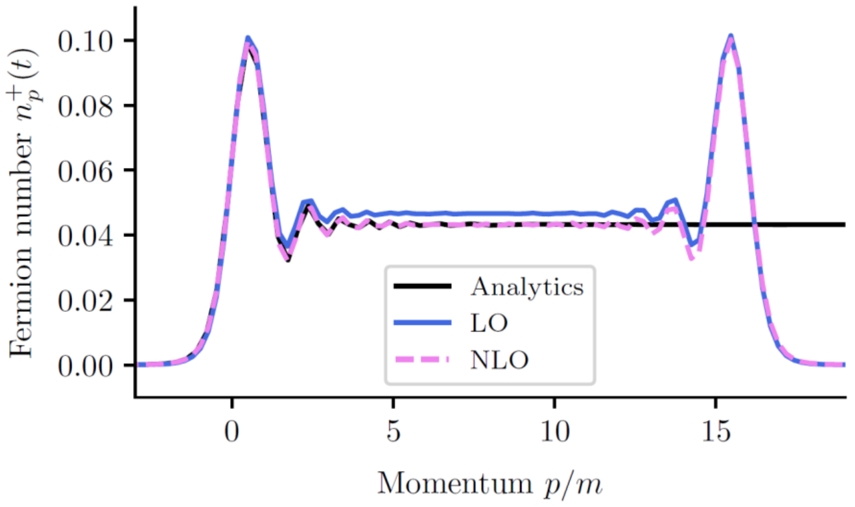

Lattice improvements (LO, NLO and NNLO below) for fermion production from initial chromoelectric field zero mode, compared to analytic one-loop predictions.

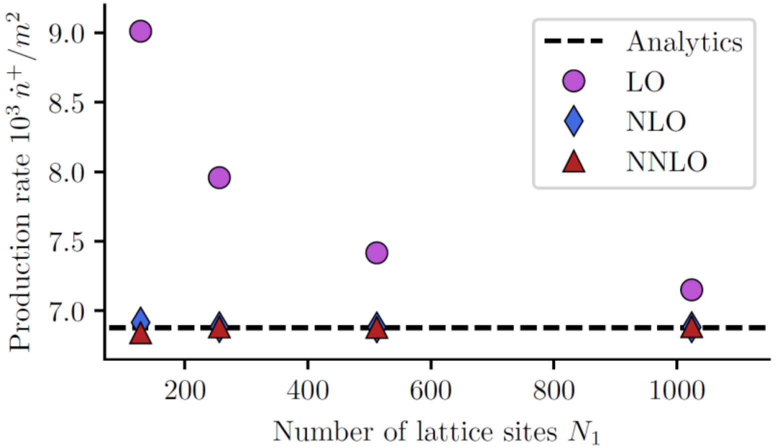

Plasma oscillations and string breaking

Plasma oscillations and string breaking

Lattice improved Hamiltonians facilitate study of plasma oscillations and string breaking, and make **computation of fourth-order correlations** feasible.

Plasma oscillations and string breaking

Lattice improved Hamiltonians facilitate study of plasma oscillations and string breaking, and make **computation of fourth-order correlations** feasible.

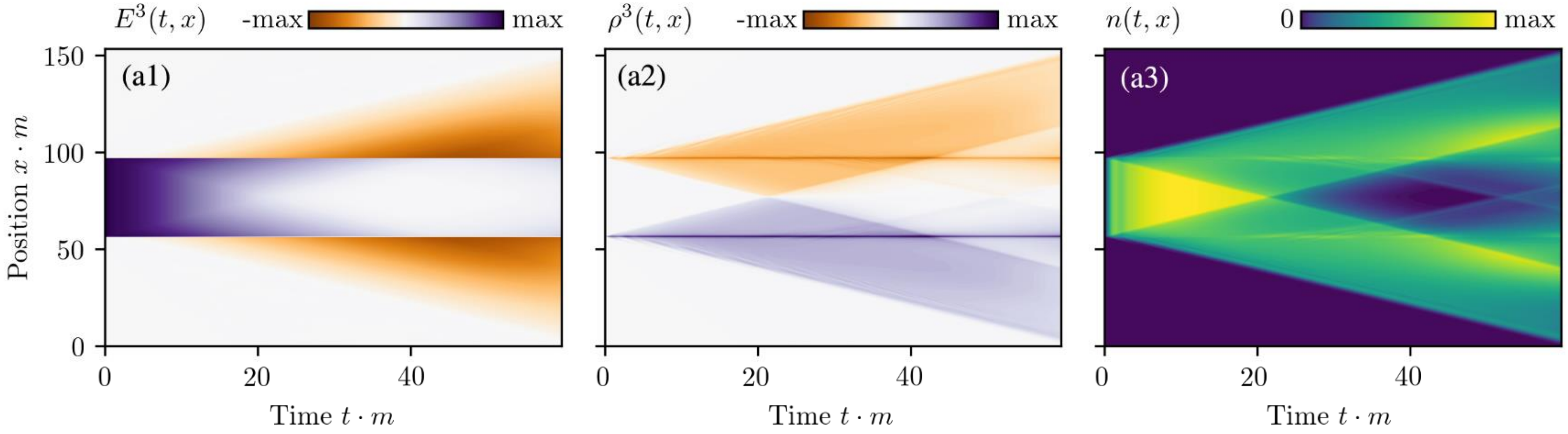

String breaking between fermion and anti-fermion: chromoelectric field, color charge, local fermion numbers (from left to right).

Plasma oscillations and string breaking

Lattice improved Hamiltonians facilitate study of plasma oscillations and string breaking, and make **computation of fourth-order correlations** feasible.

Connected color charge correlator:

$$C_{nm}^{ab}(t) = \frac{1}{2}\langle\{\rho_n^a(t), \rho_m^b(t)\}\rangle - \langle\rho_n^a(t)\rangle\langle\rho_m^b(t)\rangle$$

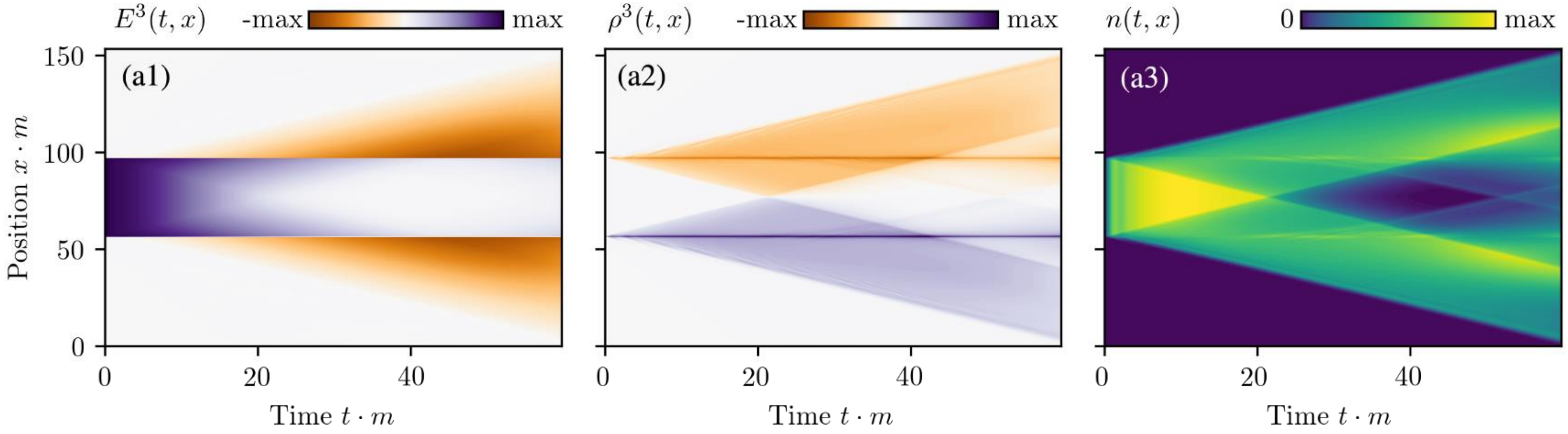

String breaking between fermion and anti-fermion: chromoelectric field, color charge, local fermion numbers (from left to right).

Plasma oscillations and string breaking

Lattice improved Hamiltonians facilitate study of plasma oscillations and string breaking, and make **computation of fourth-order correlations** feasible.

Connected color charge correlator:

$$C^{ab}_{nm}(t) = \frac{1}{2}\langle\{\rho^a_n(t), \rho^b_m(t)\}\rangle - \langle\rho^a_n(t)\rangle\langle\rho^b_m(t)\rangle$$

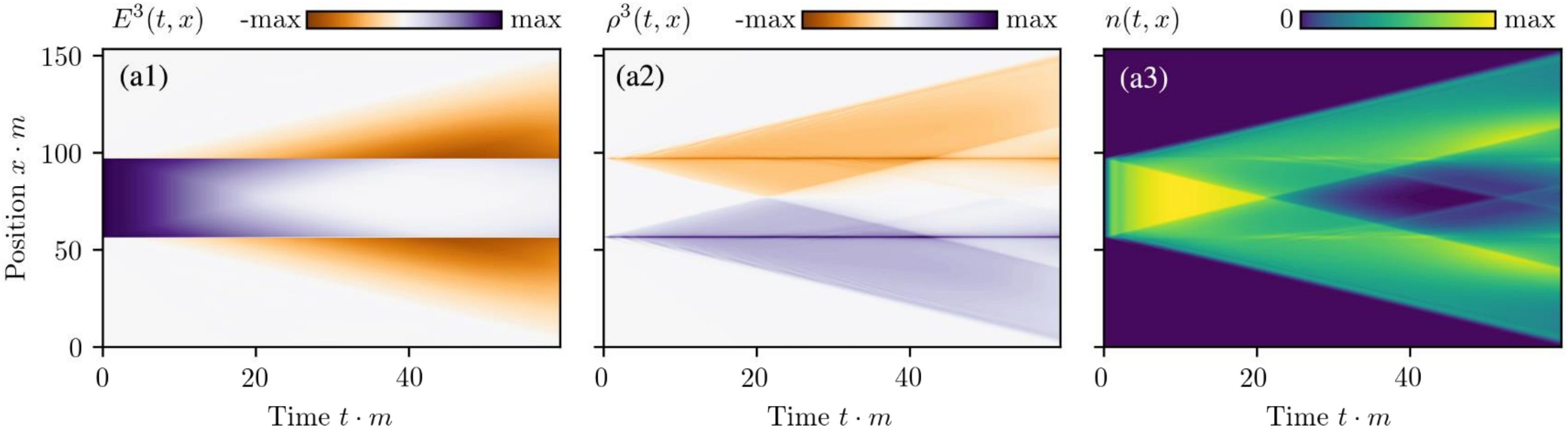

String breaking between fermion and anti-fermion: chromoelectric field, color charge, local fermion numbers (from left to right).

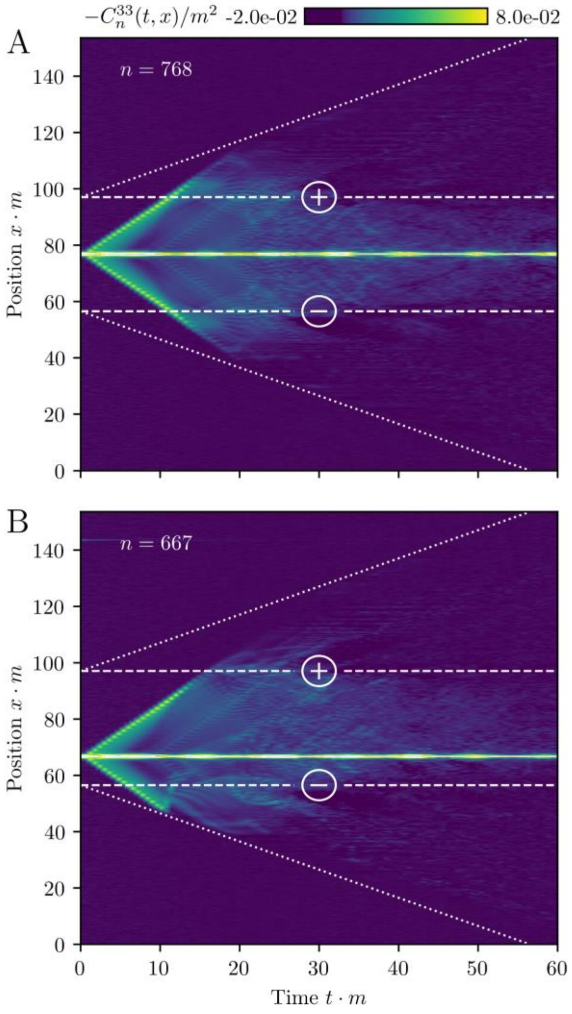

Connected charge-charge correlator in string breaking scenario.

Content

1. Lattice improved Hamiltonians for classical-statistical simulations
2. Non-thermal fixed points in persistent homology
3. Confinement in persistent homology
4. Conclusions & outlook

Alpha complexes and persistent homology

Alpha complexes and persistent homology

Start from a given point cloud $X \subseteq \mathbb{R}^n$.
Alpha complex $\alpha_r(X)$: simplicial complex (collection of simplices closed under taking boundaries), constructed from Delaunay triangulation from simplices of radius $\leq r$. [Edelsbrunner & Mücke, 1994]

Alpha complexes and persistent homology

Start from a given point cloud $X \subseteq \mathbb{R}^n$.
Alpha complex $\alpha_r(X)$: simplicial complex (collection of simplices closed under taking boundaries), constructed from Delaunay triangulation from simplices of radius $\leq r$. [Edelsbrunner & Mücke, 1994]

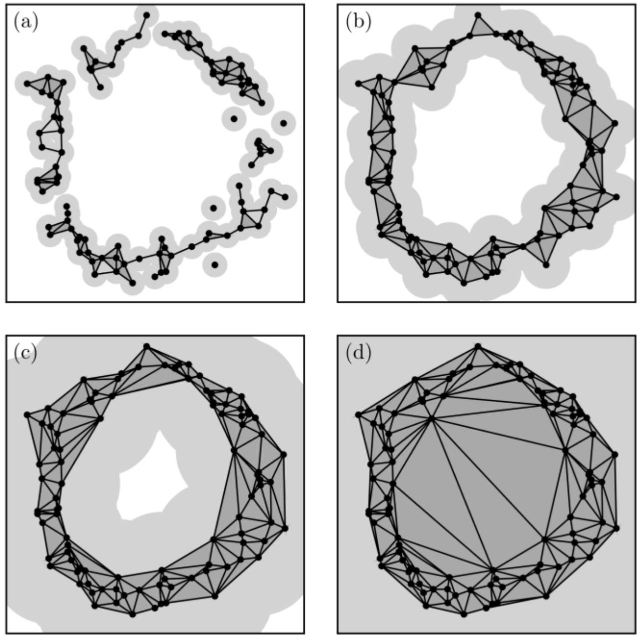

Alpha complexes of increasing radii for an approximately circular point cloud.

Alpha complexes and persistent homology

Start from a given point cloud $X \subseteq \mathbb{R}^n$.
Alpha complex $\alpha_r(X)$: simplicial complex (collection of simplices closed under taking boundaries), constructed from Delaunay triangulation from simplices of radius $\leq r$. [Edelsbrunner & Mücke, 1994]

Alpha complexes form filtration: $\alpha_r(X) \subseteq \alpha_s(X)\ \forall\ r \leq s$.

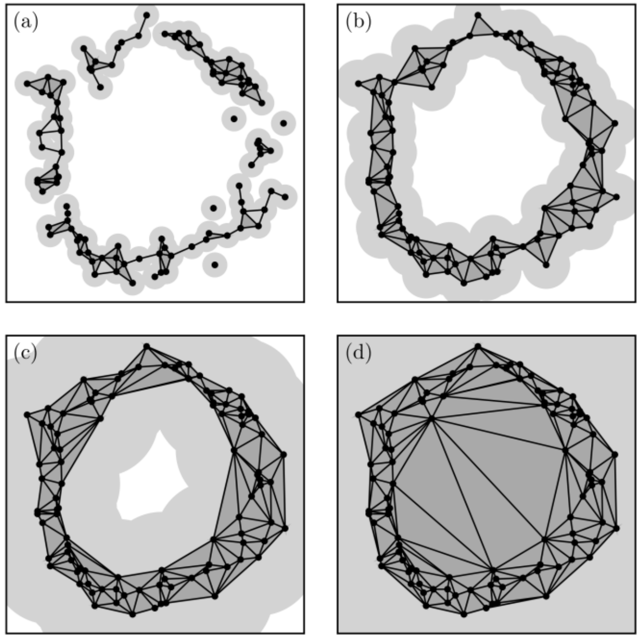

Alpha complexes of increasing radii for an approximately circular point cloud.

Alpha complexes and persistent homology

Start from a given point cloud $X \subseteq \mathbb{R}^n$.
Alpha complex $\alpha_r(X)$: simplicial complex (collection of simplices closed under taking boundaries), constructed from Delaunay triangulation from simplices of radius $\leq r$. [Edelsbrunner & Mücke, 1994]

Alpha complexes form filtration: $\alpha_r(X) \subseteq \alpha_s(X) \; \forall \, r \leq s$.

Can study their topology (homology groups), in particular its changes with the radius r, giving rise to *persistent homology:*

Holes of different dimensions can be born and can die again, as the filtration is swept through. [Edelsbrunner *et al.,* 2000; Zomorodian & Carlsson, 2004]

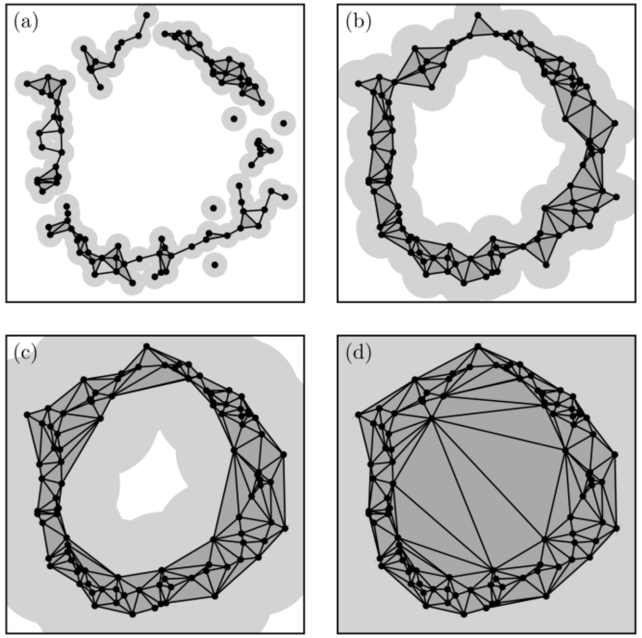

Alpha complexes of increasing radii for an approximately circular point cloud.

Alpha complexes and persistent homology

Start from a given point cloud $X \subseteq \mathbb{R}^n$.
Alpha complex $\alpha_r(X)$: simplicial complex (collection of simplices closed under taking boundaries), constructed from Delaunay triangulation from simplices of radius $\leq r$. [Edelsbrunner & Mücke, 1994]

Alpha complexes form filtration: $\alpha_r(X) \subseteq \alpha_s(X) \; \forall \; r \leq s$.

Can study their topology (homology groups), in particular its changes with the radius r, giving rise to *persistent homology:*

Holes of different dimensions can be born and can die again, as the filtration is swept through. [Edelsbrunner *et al.,* 2000; Zomorodian & Carlsson, 2004]

Crucial:

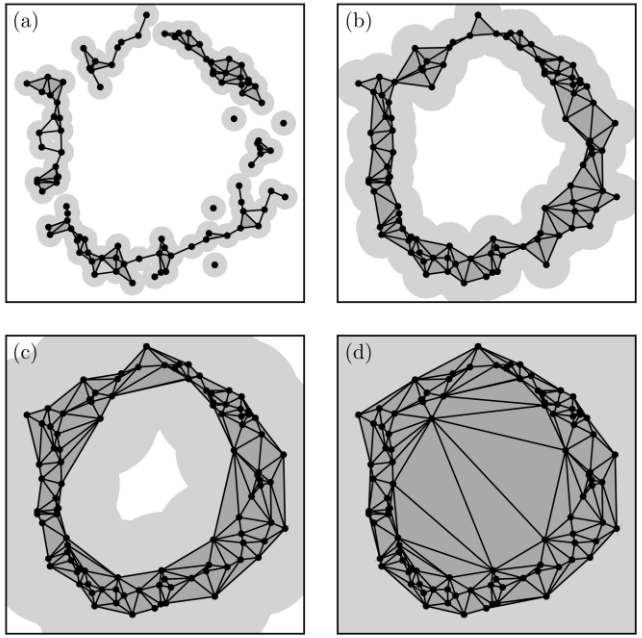

Alpha complexes of increasing radii for an approximately circular point cloud.

Alpha complexes and persistent homology

Start from a given point cloud $X \subseteq \mathbb{R}^n$.
Alpha complex $\alpha_r(X)$: simplicial complex (collection of simplices closed under taking boundaries), constructed from Delaunay triangulation from simplices of radius $\leq r$. [Edelsbrunner & Mücke, 1994]

Alpha complexes form filtration: $\alpha_r(X) \subseteq \alpha_s(X)\ \forall\, r \leq s$.

Can study their topology (homology groups), in particular its changes with the radius r, giving rise to *persistent homology:*

Holes of different dimensions can be born and can die again, as the filtration is swept through. [Edelsbrunner *et al.*, 2000; Zomorodian & Carlsson, 2004]

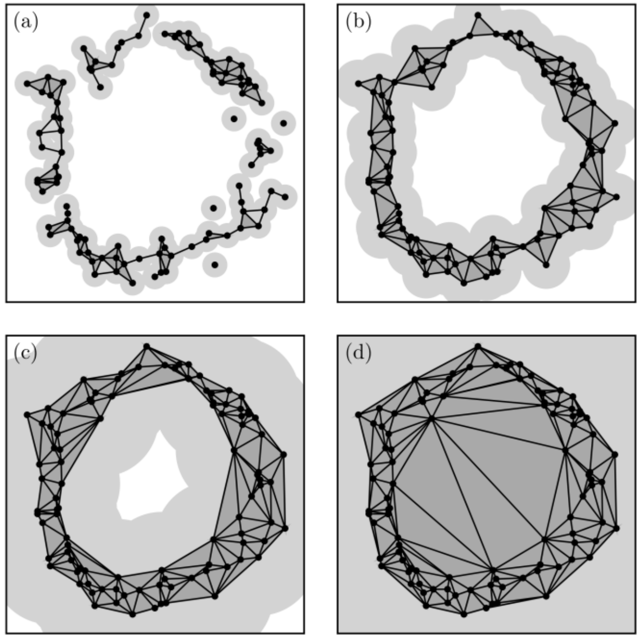

Alpha complexes of increasing radii for an approximately circular point cloud.

Crucial:
- Stability: Perturbations of X result in small changes of persistent homology. [Cohen-Steiner *et al.*, 2007 & 2010]

Alpha complexes and persistent homology

Start from a given point cloud $X \subseteq \mathbb{R}^n$.
Alpha complex $\alpha_r(X)$: simplicial complex (collection of simplices closed under taking boundaries), constructed from Delaunay triangulation from simplices of radius $\leq r$. [Edelsbrunner & Mücke, 1994]

Alpha complexes form filtration: $\alpha_r(X) \subseteq \alpha_s(X) \;\forall\; r \leq s$.

Can study their topology (homology groups), in particular its changes with the radius r, giving rise to *persistent homology:*

Holes of different dimensions can be born and can die again, as the filtration is swept through. [Edelsbrunner *et al.,* 2000; Zomorodian & Carlsson, 2004]

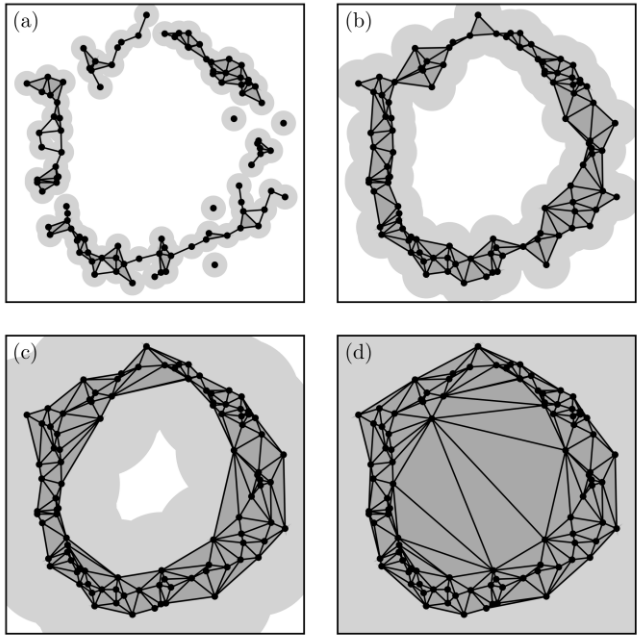

Alpha complexes of increasing radii for an approximately circular point cloud.

Crucial:
- Stability: Perturbations of X result in small changes of persistent homology. [Cohen-Steiner *et al.,* 2007 & 2010]
- Well-defined large-volume asymptotics, including notions of ergodicity. [Hiraoka *et al.*, 2018; DS & Wienhard, 2020]

Alpha complexes and persistent homology

Start from a given point cloud $X \subseteq \mathbb{R}^n$.
Alpha complex $\alpha_r(X)$: simplicial complex (collection of simplices closed under taking boundaries), constructed from Delaunay triangulation from simplices of radius $\leq r$. [Edelsbrunner & Mücke, 1994]

Alpha complexes form filtration: $\alpha_r(X) \subseteq \alpha_s(X) \; \forall \; r \leq s$.

Can study their topology (homology groups), in particular its changes with the radius r, giving rise to *persistent homology:*

Holes of different dimensions can be born and can die again, as the filtration is swept through. [Edelsbrunner *et al.,* 2000; Zomorodian & Carlsson, 2004]

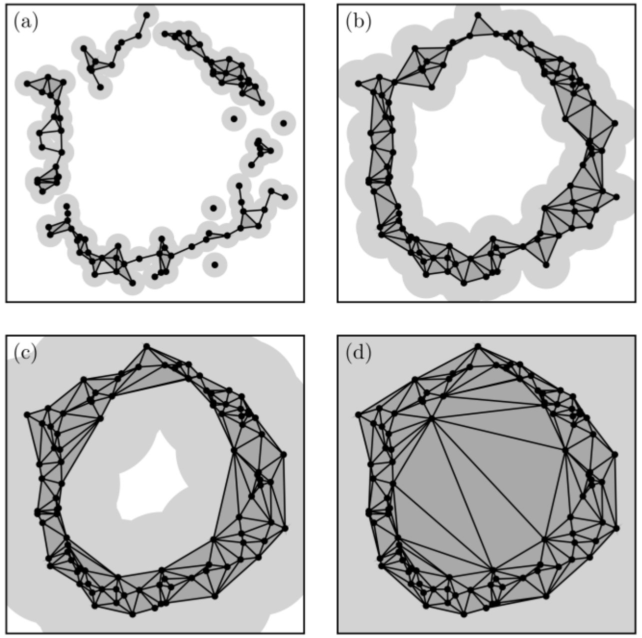

Alpha complexes of increasing radii for an approximately circular point cloud.

Crucial:
- Stability: Perturbations of X result in small changes of persistent homology. [Cohen-Steiner *et al.,* 2007 & 2010]
- Well-defined large-volume asymptotics, including notions of ergodicity. [Hiraoka *et al.*, 2018; DS & Wienhard, 2020]
- Computation facilitated by easily usable software packages such as GUDHI or Ripser

Dynamical self-similarity in persistent homology

Dynamical self-similarity in persistent homology

Sufficiently complex many-body quantum systems can exhibit nonthermal fixed points, attractors on their path towards thermal equilibrium, characterized by dynamical self-similar scaling. [Micha & Tkachev, 2004; Berges *et al.,* 2008; Prüfer *et al.,* 2018; Erne *et al.,* 2018; Eigen *et al.,* 2018]

Dynamical self-similarity in persistent homology

Sufficiently complex many-body quantum systems can exhibit nonthermal fixed points, attractors on their path towards thermal equilibrium, characterized by dynamical self-similar scaling. [Micha & Tkachev, 2004; Berges *et al.*, 2008; Prüfer *et al.*, 2018; Erne *et al.*, 2018; Eigen *et al.*, 2018]

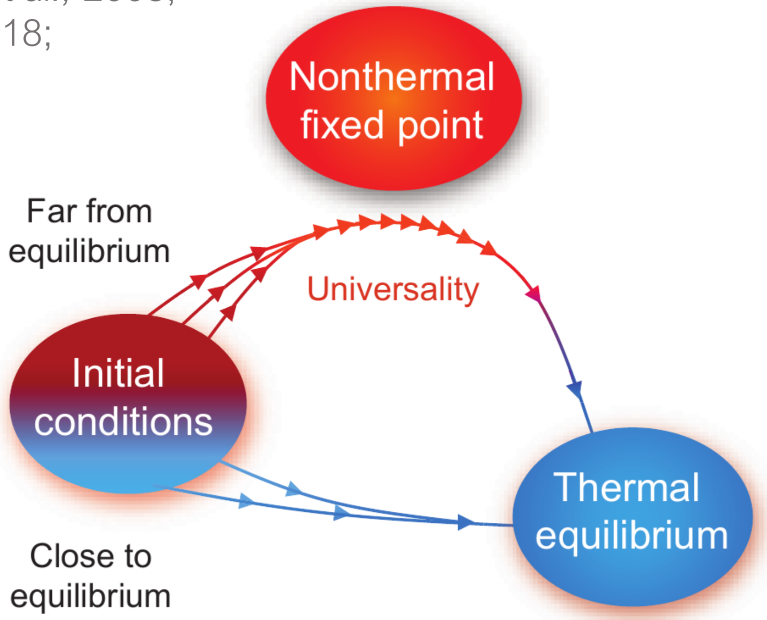

Generic path towards thermal equilibrium [Berges 2015].

Dynamical self-similarity in persistent homology

Sufficiently complex many-body quantum systems can exhibit nonthermal fixed points, attractors on their path towards thermal equilibrium, characterized by dynamical self-similar scaling. [Micha & Tkachev, 2004; Berges *et al.*, 2008; Prüfer *et al.*, 2018; Erne *et al.*, 2018; Eigen *et al.*, 2018]

Experiments can probe thermalization of quantum systems in detail.

[e.g., Prüfer, DS, *et al.*, 2022]

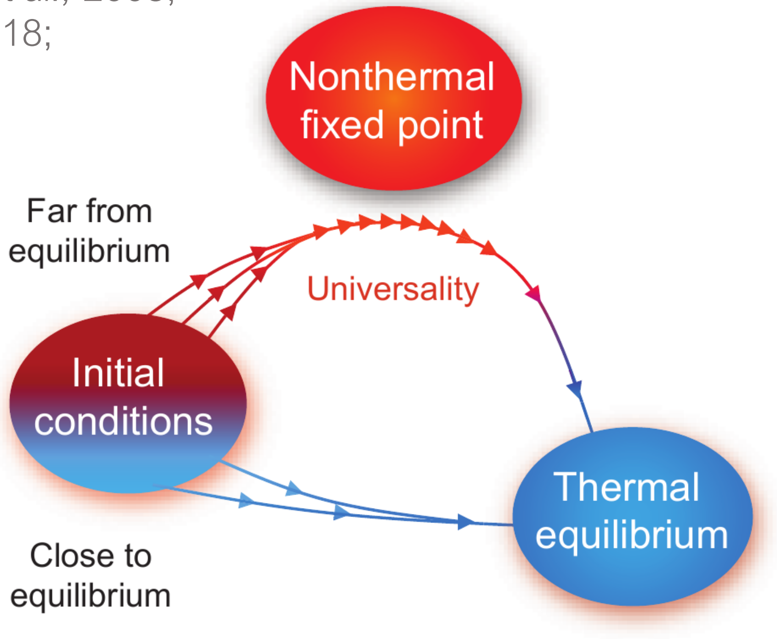

Generic path towards thermal equilibrium [Berges 2015].

Dynamical self-similarity in persistent homology

Sufficiently complex many-body quantum systems can exhibit nonthermal fixed points, attractors on their path towards thermal equilibrium, characterized by dynamical self-similar scaling. [Micha & Tkachev, 2004; Berges *et al.*, 2008; Prüfer *et al.*, 2018; Erne *et al.*, 2018; Eigen *et al.*, 2018]

Experiments can probe thermalization of quantum systems in detail. [e.g., Prüfer, DS, *et al.*, 2022]

Universal behavior across initial conditions and theories, demanding for refined classification schemes. [Berges *et al.*, 2014 & 2015; Orioli *et al.*, 2015]

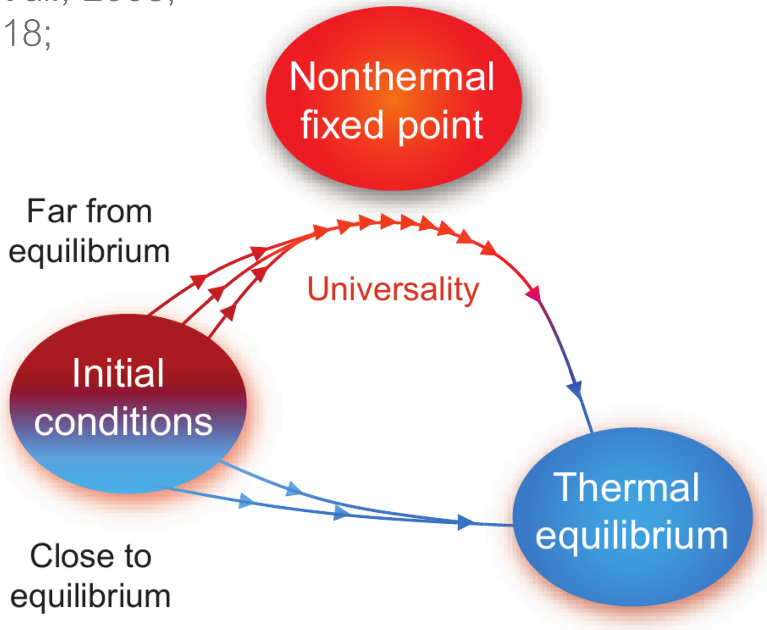

Generic path towards thermal equilibrium [Berges 2015].

Dynamical self-similarity in persistent homology

Sufficiently complex many-body quantum systems can exhibit nonthermal fixed points, attractors on their path towards thermal equilibrium, characterized by dynamical self-similar scaling. [Micha & Tkachev, 2004; Berges *et al.*, 2008; Prüfer *et al.*, 2018; Erne *et al.*, 2018; Eigen *et al.*, 2018]

Experiments can probe thermalization of quantum systems in detail. [e.g., Prüfer, DS, *et al.*, 2022]

Universal behavior across initial conditions and theories, demanding for refined classification schemes. [Berges *et al.*, 2014 & 2015; Orioli *et al.*, 2015]

Usually study correlation functions up to high orders. [Schweigler *et al.*, 2015]

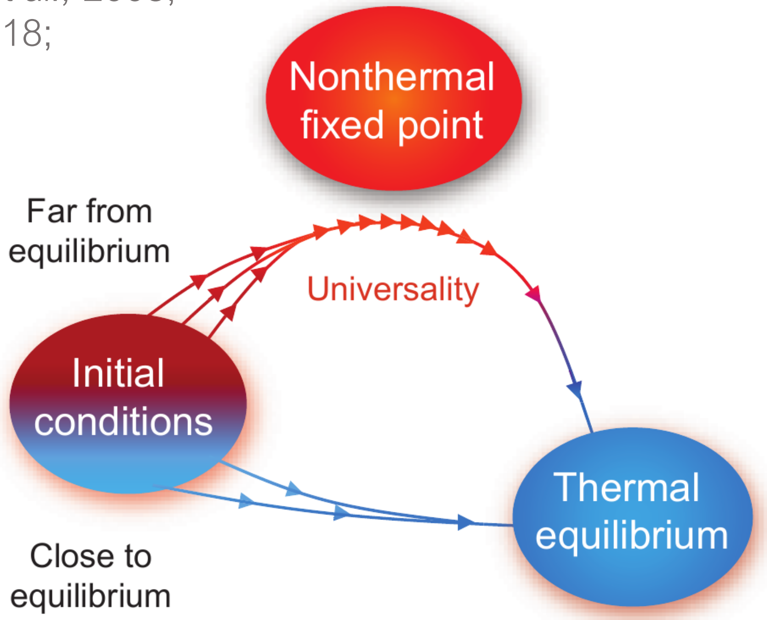

Generic path towards thermal equilibrium [Berges 2015].

Dynamical self-similarity in persistent homology

Sufficiently complex many-body quantum systems can exhibit nonthermal fixed points, attractors on their path towards thermal equilibrium, characterized by dynamical self-similar scaling. [Micha & Tkachev, 2004; Berges *et al.*, 2008; Prüfer *et al.*, 2018; Erne *et al.*, 2018; Eigen *et al.*, 2018]

Experiments can probe thermalization of quantum systems in detail. [e.g., Prüfer, DS, *et al.*, 2022]

Universal behavior across initial conditions and theories, demanding for refined classification schemes. [Berges *et al.*, 2014 & 2015; Orioli *et al.*, 2015]

Usually study correlation functions up to high orders. [Schweigler *et al.*, 2015]

Can non-local, geometric and topological structures help?

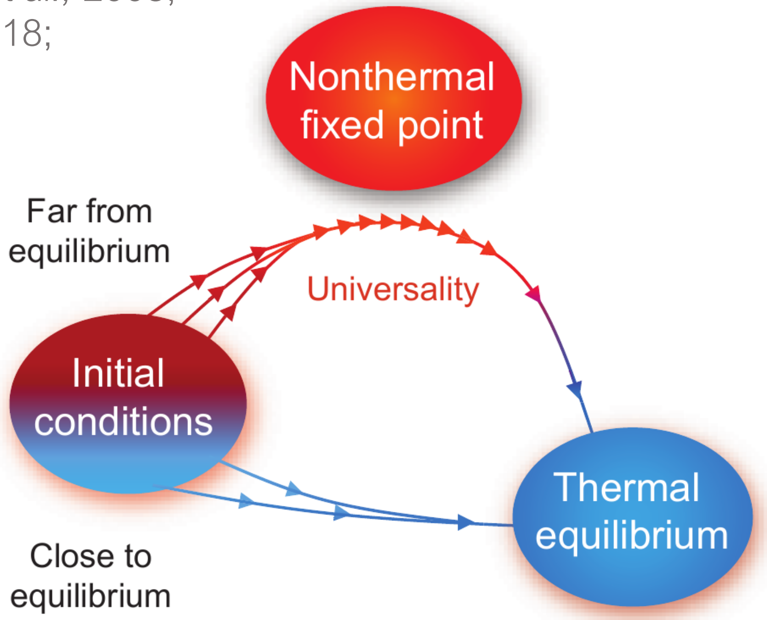

Generic path towards thermal equilibrium [Berges 2015].

Dynamical self-similarity in persistent homology

Dynamical self-similarity in persistent homology

First study via non-relativistic, dilute Bose gas in a plane. Accurately described in class.-stat. regime by Gross-Pitaevskii equation, which is numerically solved on a spatial lattice: [Orioli *et al.*, 2015]

$$i\partial_t \psi(t,\mathbf{x}) = \left(-\frac{\nabla^2}{2m} + g|\psi(t,\mathbf{x})|^2\right)\psi(t,\mathbf{x})$$

Dynamical self-similarity in persistent homology

First study via non-relativistic, dilute Bose gas in a plane. Accurately described in class.-stat. regime by Gross-Pitaevskii equation, which is numerically solved on a spatial lattice: [Orioli *et al.*, 2015]

$$i\partial_t \psi(t,\mathbf{x}) = \left(-\frac{\nabla^2}{2m} + g|\psi(t,\mathbf{x})|^2\right)\psi(t,\mathbf{x})$$

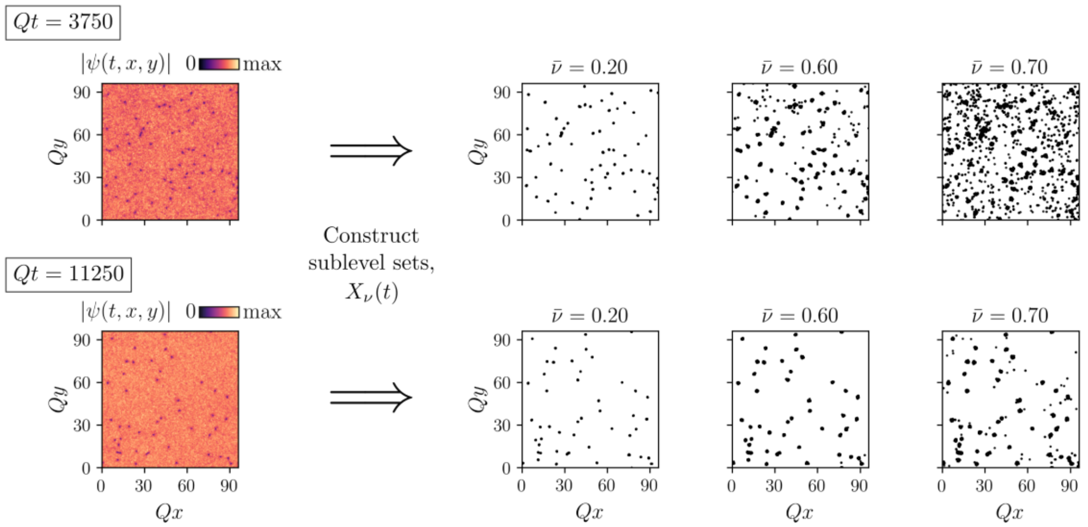

Point cloud generation via amplitude sublevel sets
[DS, Berges, Oberthaler, Wienhard, 2021].

Dynamical self-similarity in persistent homology

First study via non-relativistic, dilute Bose gas in a plane. Accurately described in class.-stat. regime by Gross-Pitaevskii equation, which is numerically solved on a spatial lattice: [Orioli *et al.*, 2015]

$$i\partial_t \psi(t,\mathbf{x}) = \left(-\frac{\nabla^2}{2m} + g|\psi(t,\mathbf{x})|^2\right)\psi(t,\mathbf{x})$$

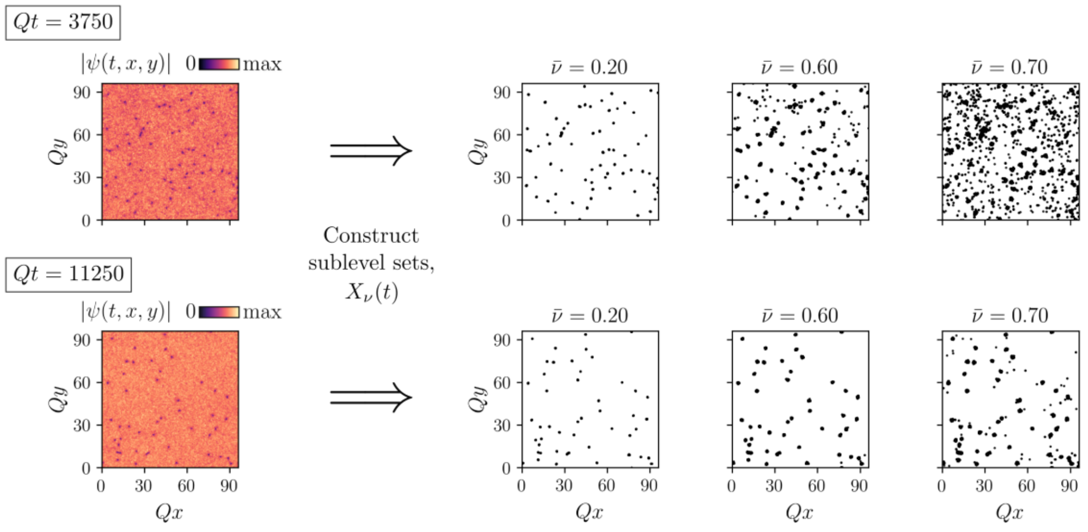

Point cloud generation via amplitude sublevel sets [DS, Berges, Oberthaler, Wienhard, 2021].

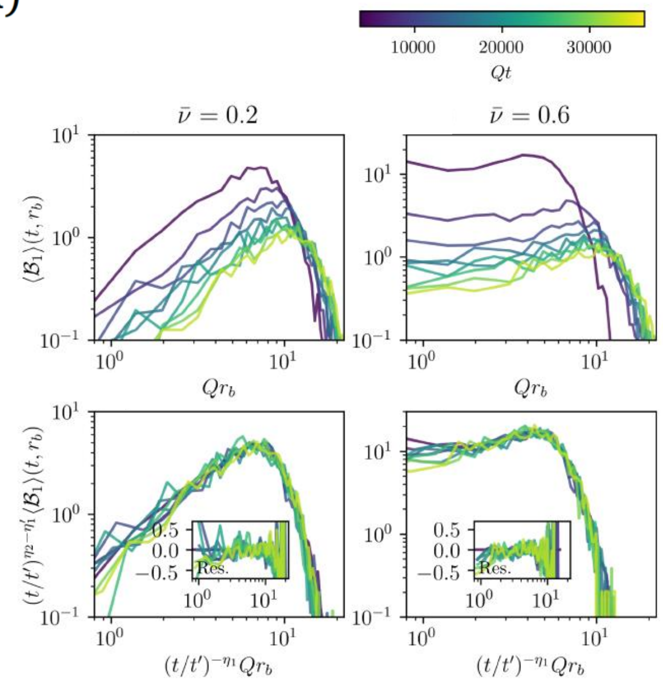

Birth statistics of holes

Dynamical self-similarity in persistent homology

Dynamical self-similarity in persistent homology

Proposed scaling ansatz for persistent homology kernel: [DS, Berges, Oberthaler, Wienhard, 2021]

$$\langle\mathfrak{P}_\ell\rangle(t, r_b, r_d) = (t/t')^{-\eta_2}\langle\mathfrak{P}_\ell\rangle(t', (t/t')^{-\eta_1} r_b, (t/t')^{-\eta_1'} r_d)$$

Dynamical self-similarity in persistent homology

Proposed scaling ansatz for persistent homology kernel: [DS, Berges, Oberthaler, Wienhard, 2021]

$$\langle \mathfrak{P}_\ell \rangle (t, r_b, r_d) = (t/t')^{-\eta_2} \langle \mathfrak{P}_\ell \rangle (t', (t/t')^{-\eta_1} r_b, (t/t')^{-\eta_1'} r_d)$$

Describes power-law blow-up of persistence length scales (sizes of topological features) in time, for instance:

$$\langle r_{d,\ell,\max} \rangle (t) = (t/t')^{\eta_1} \langle r_{d,\ell,\max} \rangle (t')$$

Dynamical self-similarity in persistent homology

Proposed scaling ansatz for persistent homology kernel: [DS, Berges, Oberthaler, Wienhard, 2021]

$$\langle \mathfrak{P}_\ell \rangle (t, r_b, r_d) = (t/t')^{-\eta_2} \langle \mathfrak{P}_\ell \rangle (t', (t/t')^{-\eta_1} r_b, (t/t')^{-\eta_1'} r_d)$$

Describes power-law blow-up of persistence length scales (sizes of topological features) in time, for instance:

$$\langle r_{d,\ell,\max} \rangle (t) = (t/t')^{\eta_1} \langle r_{d,\ell,\max} \rangle (t')$$

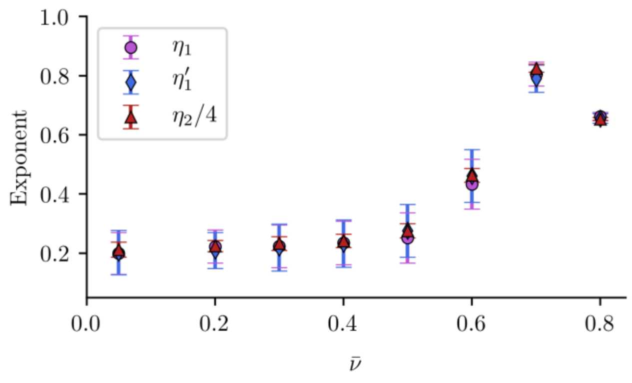

Found **scaling exponent spectrum.**

Dynamical self-similarity in persistent homology

Proposed scaling ansatz for persistent homology kernel: [DS, Berges, Oberthaler, Wienhard, 2021]

$$\langle \mathfrak{P}_\ell \rangle (t, r_b, r_d) = (t/t')^{-\eta_2} \langle \mathfrak{P}_\ell \rangle (t', (t/t')^{-\eta_1} r_b, (t/t')^{-\eta_1'} r_d)$$

Describes power-law blow-up of persistence length scales (sizes of topological features) in time, for instance:

$$\langle r_{d,\ell,\max} \rangle (t) = (t/t')^{\eta_1} \langle r_{d,\ell,\max} \rangle (t')$$

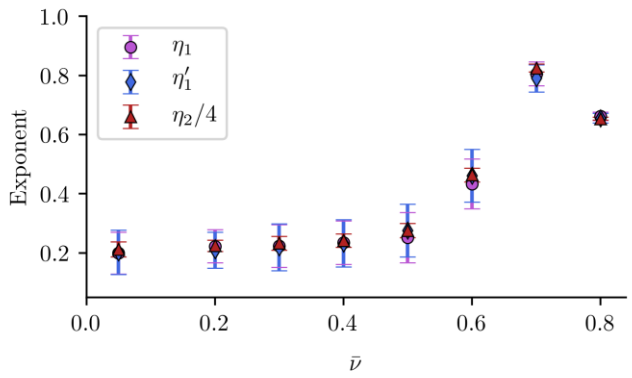

Found **scaling exponent spectrum**.

Exponent 0.2 known from correlations.

[Simula *et al.*, 2014; Karl & Gasenzer, 2017; Deng *et al.*, 2018]

Dynamical self-similarity in persistent homology

Proposed scaling ansatz for persistent homology kernel: [DS, Berges, Oberthaler, Wienhard, 2021]

$$\langle \mathfrak{P}_\ell \rangle(t, r_b, r_d) = (t/t')^{-\eta_2} \langle \mathfrak{P}_\ell \rangle(t', (t/t')^{-\eta_1} r_b, (t/t')^{-\eta_1'} r_d)$$

Describes power-law blow-up of persistence length scales (sizes of topological features) in time, for instance:

$$\langle r_{d,\ell,\max} \rangle(t) = (t/t')^{\eta_1} \langle r_{d,\ell,\max} \rangle(t')$$

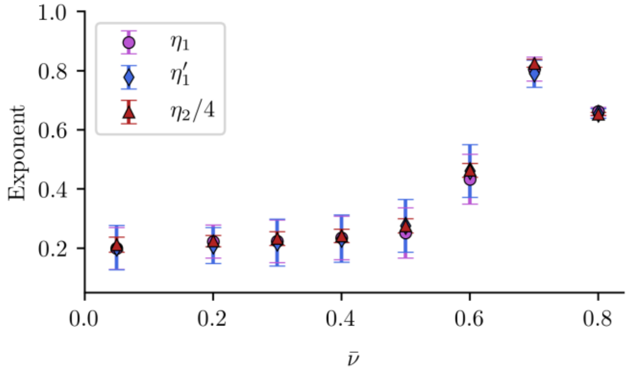

Found **scaling exponent spectrum**.

Exponent 0.2 known from correlations.

[Simula *et al.*, 2014; Karl & Gasenzer, 2017; Deng *et al.*, 2018]

Peak new, refining universality?

Dynamical self-similarity in persistent homology

Proposed scaling ansatz for persistent homology kernel: [DS, Berges, Oberthaler, Wienhard, 2021]

$$\langle \mathfrak{P}_\ell \rangle (t, r_b, r_d) = (t/t')^{-\eta_2} \langle \mathfrak{P}_\ell \rangle (t', (t/t')^{-\eta_1} r_b, (t/t')^{-\eta_1'} r_d)$$

Describes power-law blow-up of persistence length scales (sizes of topological features) in time, for instance:

$$\langle r_{d,\ell,\max} \rangle (t) = (t/t')^{\eta_1} \langle r_{d,\ell,\max} \rangle (t')$$

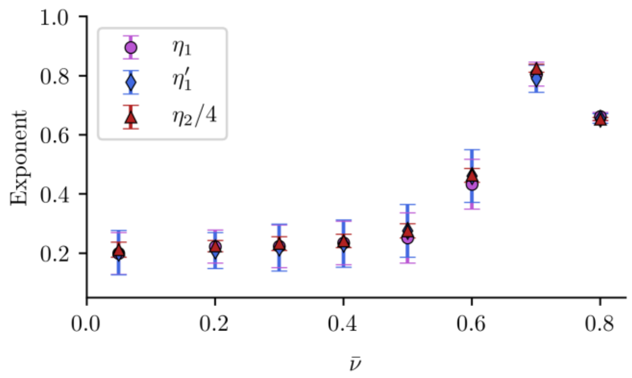

Found **scaling exponent spectrum.**

Exponent 0.2 known from correlations.

[Simula *et al.*, 2014; Karl & Gasenzer, 2017; Deng *et al.*, 2018]

Peak new, refining universality?

Why $\eta_2 = 4\eta_1$?

Packing relation from point process theory and random PH

Packing relation from point process theory and random PH

Found numerically in different simulations that for different spatial dimensions d the relation

$$\eta_2 = (2 + d)\eta_1$$

holds as a manifestation of a constant system volume bounding the number of homology classes.

Packing relation from point process theory and random PH

Found numerically in different simulations that for different spatial dimensions d the relation

$$\eta_2 = (2 + d)\eta_1$$

holds as a manifestation of a constant system volume bounding the number of homology classes.

Have proven this **packing relation** rigorously using the theory of point processes, via the notion of bounded total persistence. [Daley & Vere-Jones, 2003 & 2008; Cohen-Steiner *et al.,* 2010; DS & Wienhard, 2021]

Packing relation from point process theory and random PH

Found numerically in different simulations that for different spatial dimensions d the relation

$$\eta_2 = (2 + d)\eta_1$$

holds as a manifestation of a constant system volume bounding the number of homology classes.

Have proven this **packing relation** rigorously using the theory of point processes, via the notion of bounded total persistence. [Daley & Vere-Jones, 2003 & 2008; Cohen-Steiner *et al.,* 2010; DS & Wienhard, 2021]

Aside, we

Packing relation from point process theory and random PH

Found numerically in different simulations that for different spatial dimensions d the relation

$$\eta_2 = (2 + d)\eta_1$$

holds as a manifestation of a constant system volume bounding the number of homology classes.

Have proven this **packing relation** rigorously using the theory of point processes, via the notion of bounded total persistence. [Daley & Vere-Jones, 2003 & 2008; Cohen-Steiner *et al.,* 2010; DS & Wienhard, 2021]

Aside, we

- introduced notions of ergodicity and intensive/extensive functional summaries to persistent homology,

Packing relation from point process theory and random PH

Found numerically in different simulations that for different spatial dimensions d the relation

$$\eta_2 = (2 + d)\eta_1$$

holds as a manifestation of a constant system volume bounding the number of homology classes.

Have proven this **packing relation** rigorously using the theory of point processes, via the notion of bounded total persistence. [Daley & Vere-Jones, 2003 & 2008; Cohen-Steiner *et al.*, 2010; DS & Wienhard, 2021]

Aside, we

- introduced notions of ergodicity and intensive/extensive functional summaries to persistent homology,
- formalized self-similar scaling for persistence diagram expectation measures,

Packing relation from point process theory and random PH

Found numerically in different simulations that for different spatial dimensions d the relation

$$\eta_2 = (2 + d)\eta_1$$

holds as a manifestation of a constant system volume bounding the number of homology classes.

Have proven this **packing relation** rigorously using the theory of point processes, via the notion of bounded total persistence. [Daley & Vere-Jones, 2003 & 2008; Cohen-Steiner *et al.*, 2010; DS & Wienhard, 2021]

Aside, we

- introduced notions of ergodicity and intensive/extensive functional summaries to persistent homology,
- formalized self-similar scaling for persistence diagram expectation measures,
- generalized a strong law of large numbers for persistent Betti numbers on asymptotically large cubes to arbitrary convex averaging sequences. [Hiraoka *et al.*, 2018]

Content

1. Lattice improved Hamiltonians for classical-statistical simulations
2. Non-thermal fixed points in persistent homology
3. Confinement in persistent homology
4. Conclusions & outlook

SU(2) lattice gauge theory simulations

SU(2) lattice gauge theory simulations

Goal: Can we gauge-invariantly and without a bias towards particular field configurations observe properties of excitations related to confinement via persistent homology?

[DS, Urban, Pawlowski, 2022]

SU(2) lattice gauge theory simulations

Goal: Can we gauge-invariantly and without a bias towards particular field configurations observe properties of excitations related to confinement via persistent homology?

[DS, Urban, Pawlowski, 2022]

Carried out **Hybrid Monte Carlo simulations** on 4d Euclidean $32^3 \times 8$ lattice with periodic boundary conditions. No gauge fixing applied. Samples are SU(2)-valued links $U_\mu(x)$, following Wilson action, $\beta = 1/g^2$:

$$S[U] = \frac{\beta}{2} \sum_{x\in\Lambda} \sum_{\mu<\nu} \mathrm{Tr}[1 - U_{\mu\nu}(x)]$$

[Duane *et al*., 1987; Gattringer & Lang 2010]

SU(2) lattice gauge theory simulations

Goal: Can we gauge-invariantly and without a bias towards particular field configurations observe properties of excitations related to confinement via persistent homology?

[DS, Urban, Pawlowski, 2022]

Carried out **Hybrid Monte Carlo simulations** on 4d Euclidean $32^3 \times 8$ lattice with periodic boundary conditions. No gauge fixing applied. Samples are SU(2)-valued links $U_\mu(x)$, following Wilson action, $\beta = 1/g^2$:

$$S[U] = \frac{\beta}{2} \sum_{x\in\Lambda} \sum_{\mu<\nu} \mathrm{Tr}[1 - U_{\mu\nu}(x)]$$

[Duane *et al.*, 1987; Gattringer & Lang 2010]

Compare multiple times to **cooled configurations** (partially removed UV fluctuations), using standard gradient flow: [Lüscher, 2010]

$$\partial_t U_\mu(x,t) = -g^2(\partial_{x,\mu} S[U(t)])U_\mu(x,t)$$

with ini. cond. $U_\mu(x,0)$ given by sampled field configuration without cooling.

Common pheno of SU(2) confinement

Common pheno of SU(2) confinement

Theory is confining at low β as signalled by zero Polyakov loop:

$$P(\mathbf{x}) := \frac{1}{2}\mathrm{Tr}\ \mathrm{P}\prod_{\tau=1}^{N_\tau} U_4(\mathbf{x},\tau), \qquad L := \frac{1}{N_\sigma^3}\langle|\sum_{\mathbf{x}\in\Lambda_s} P(\mathbf{x})|\rangle$$

Common pheno of SU(2) confinement

Theory is confining at low β as signalled by zero Polyakov loop:

$$P(\mathbf{x}) := \frac{1}{2}\mathrm{Tr}\ \mathrm{P}\prod_{\tau=1}^{N_\tau} U_4(\mathbf{x},\tau), \qquad L := \frac{1}{N_\sigma^3}\langle|\sum_{\mathbf{x}\in\Lambda_s} P(\mathbf{x})|\rangle$$

Spontaneous center symmetry breaking in Polyakov loop traces above $\beta_c \simeq 2.3$:

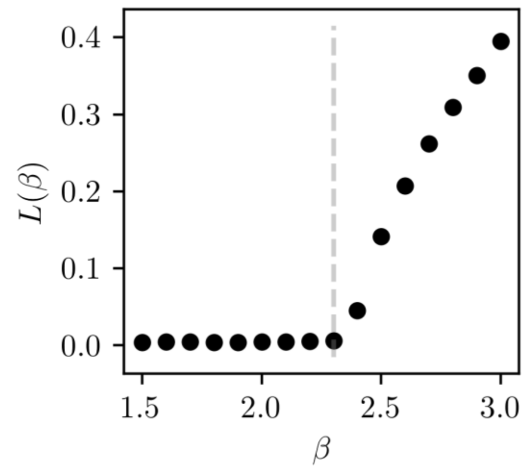

Common pheno of SU(2) confinement

Theory is confining at low β as signalled by zero Polyakov loop:

$$P(\mathbf{x}) := \frac{1}{2}\mathrm{Tr}\ \mathrm{P}\prod_{\tau=1}^{N_\tau} U_4(\mathbf{x},\tau), \qquad L := \frac{1}{N_\sigma^3}\langle|\sum_{\mathbf{x}\in\Lambda_s} P(\mathbf{x})|\rangle$$

Spontaneous center symmetry breaking in Polyakov loop traces above $\beta_c \simeq 2.3$:

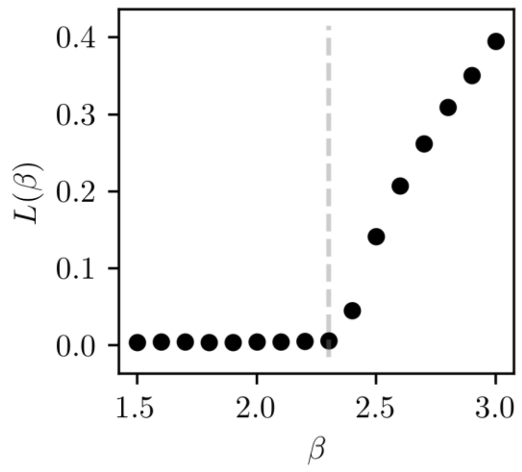

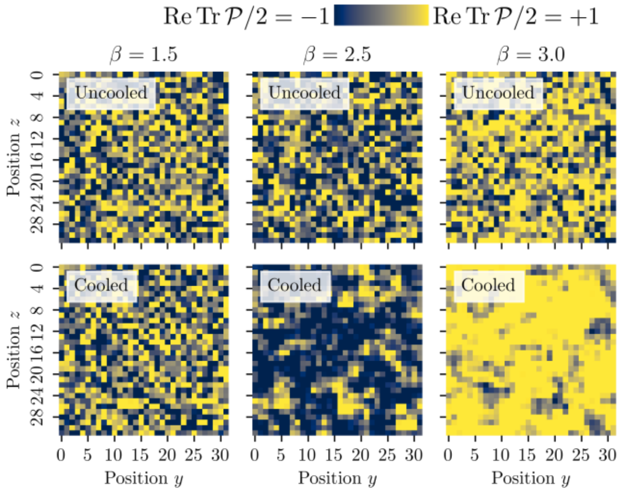

Common pheno of SU(2) confinement

Theory is confining at low β as signalled by zero Polyakov loop:

$$P(\mathbf{x}) := \frac{1}{2}\mathrm{Tr}\,\mathrm{P}\prod_{\tau=1}^{N_\tau} U_4(\mathbf{x},\tau), \qquad L := \frac{1}{N_\sigma^3}\langle|\sum_{\mathbf{x}\in\Lambda_s} P(\mathbf{x})|\rangle$$

Spontaneous center symmetry breaking in Polyakov loop traces above $\beta_c \simeq 2.3$:

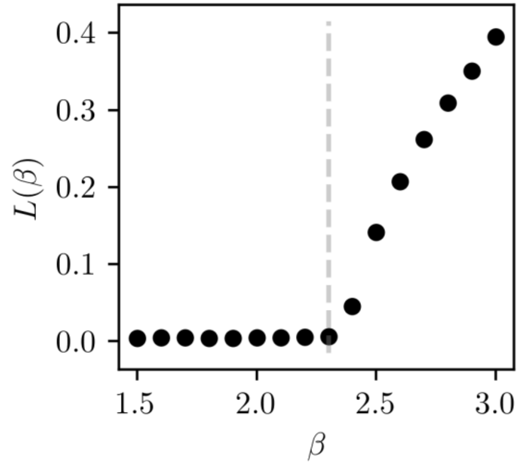

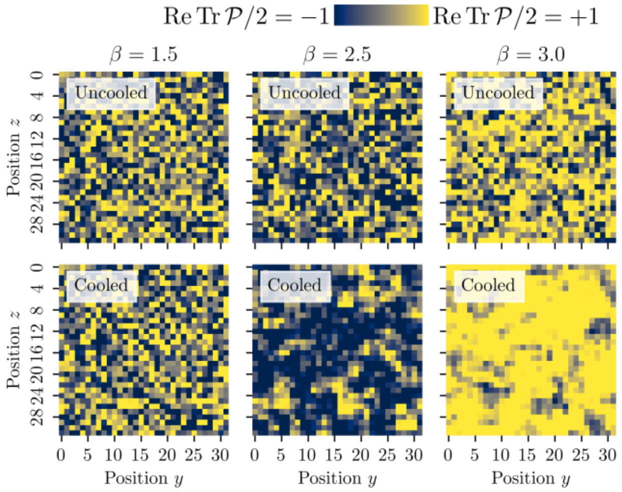

Evidence for driving via topological excitations, require interactions with Polyakov loops.
Monopole constituents of calorons, **instanton-dyons**, yield non-trivial Polyakov loops at infinity.
Ensembles can account for confinement in theories with trivial gauge group center.

[Kraan & van Baal 1998; Lee & Lu 1998; Diakonov & Petrov, 2011]

Confinement features from different filtrations

Confinement features from different filtrations

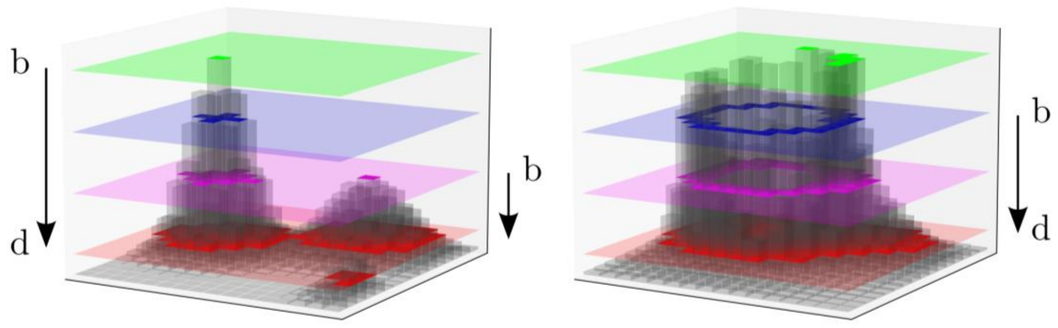

PH of cubical complex superlevel sets, dim. 0 (left), dim. 1 (right).

Confinement features from different filtrations

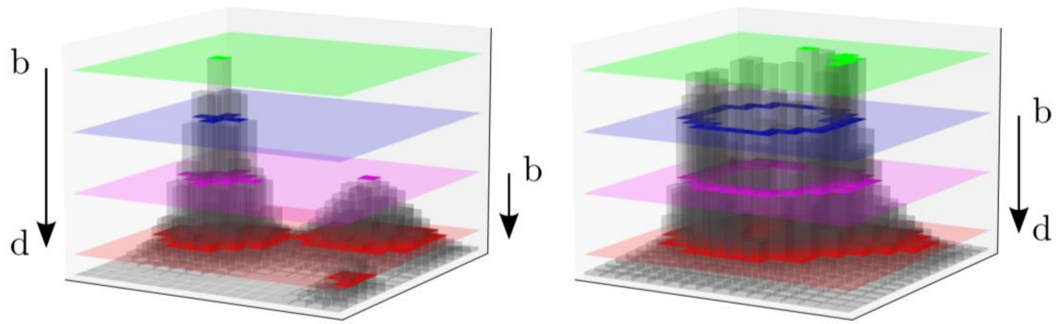

PH of cubical complex superlevel sets, dim. 0 (left), dim. 1 (right).

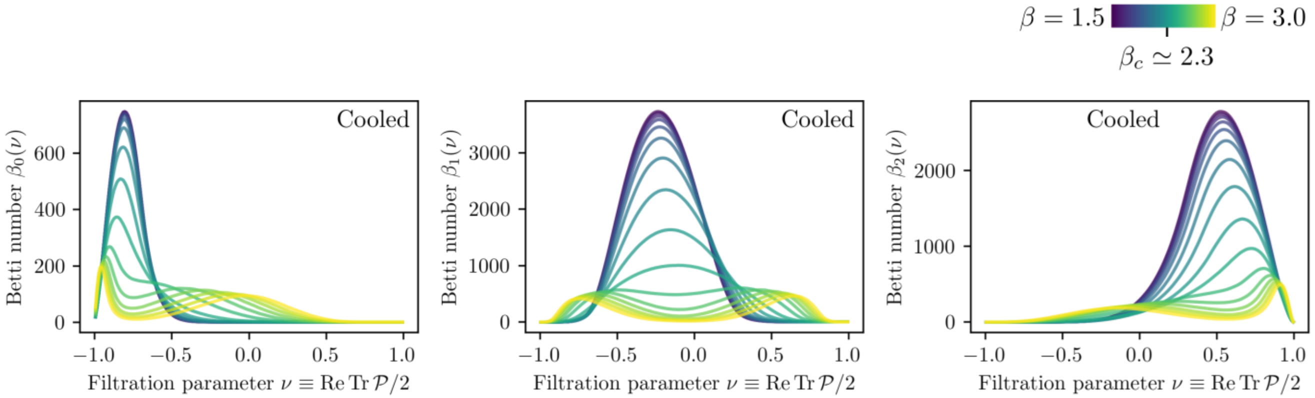

Spontaneously broken center symmetry in Polyakov loop sublevel sets.

Confinement features from different filtrations

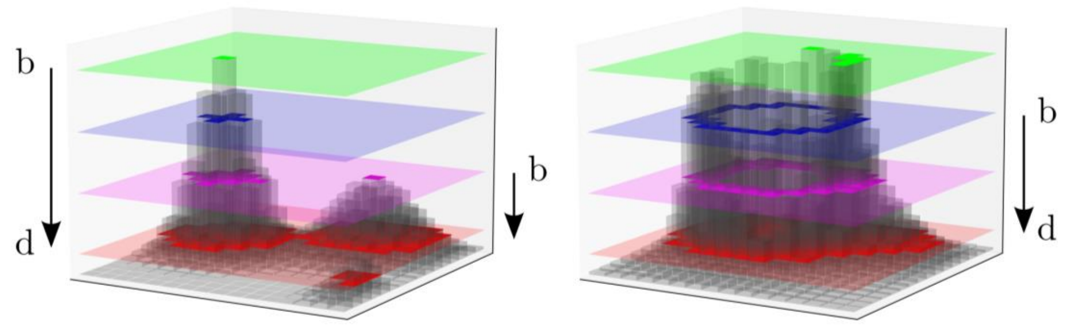

PH of cubical complex superlevel sets, dim. 0 (left), dim. 1 (right).

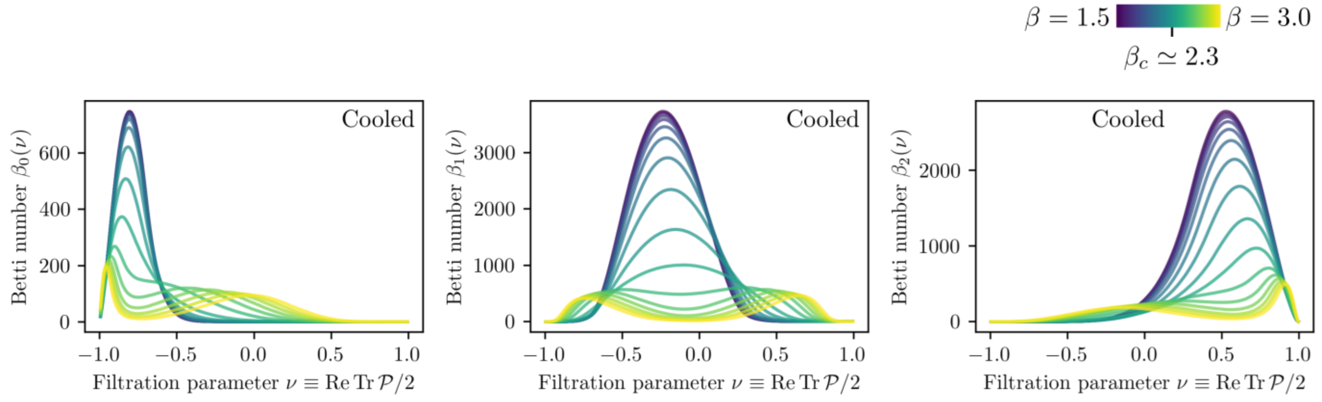

Spontaneously broken center symmetry in Polyakov loop sublevel sets.

Usual topological density $q \sim \mathrm{Tr}\,\mathbf{E}\cdot\mathbf{B}$ often contains strong UV fluctuation signatures. Rewrite top. charge as integral over 3-torus with integrand the Polyakov loop top. density: $q_{\mathcal{P}}(\mathbf{x}) := \frac{1}{24\pi^2}\varepsilon_{ijk}\mathrm{Tr}[(\mathcal{P}^{-1}\partial_i\mathcal{P})(\mathcal{P}^{-1}\partial_j\mathcal{P})(\mathcal{P}^{-1}\partial_k\mathcal{P})]$ [Ford *et al.*, 1998]

Confinement features from different filtrations

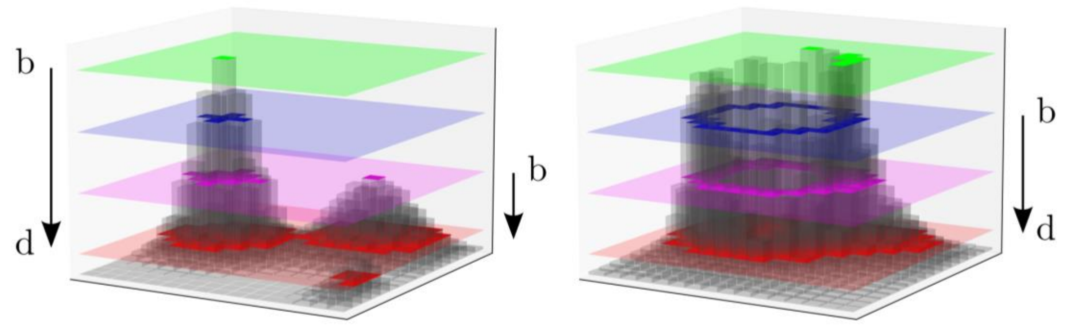

PH of cubical complex superlevel sets, dim. 0 (left), dim. 1 (right).

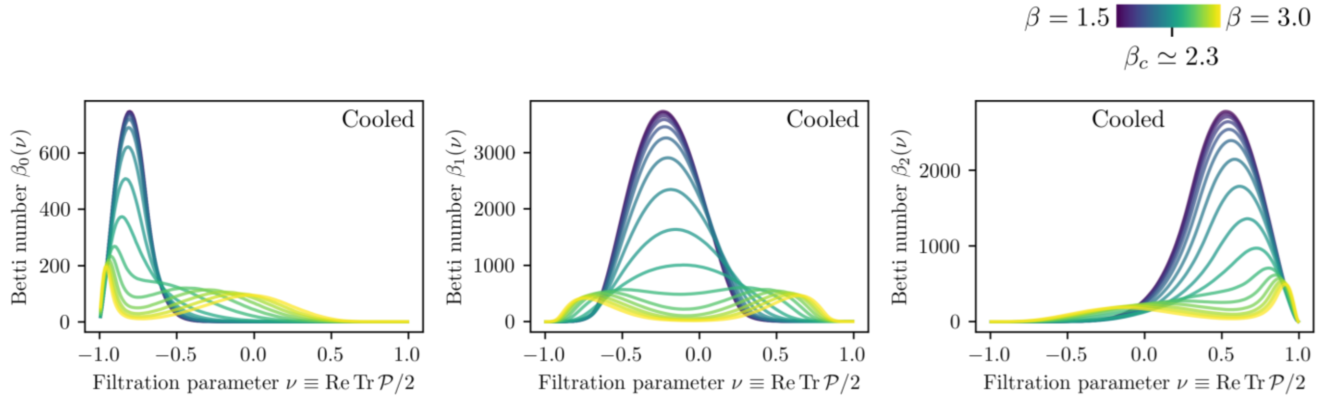

Spontaneously broken center symmetry in Polyakov loop sublevel sets.

Usual topological density $q \sim \mathrm{Tr}\,\mathbf{E} \cdot \mathbf{B}$ often contains strong UV fluctuation signatures. Rewrite top. charge as integral over 3-torus with integrand the Polyakov loop top. density: $q_{\mathcal{P}}(\mathbf{x}) := \frac{1}{24\pi^2}\varepsilon_{ijk}\mathrm{Tr}[(\mathcal{P}^{-1}\partial_i\mathcal{P})(\mathcal{P}^{-1}\partial_j\mathcal{P})(\mathcal{P}^{-1}\partial_k\mathcal{P})]$ [Ford *et al.*, 1998]

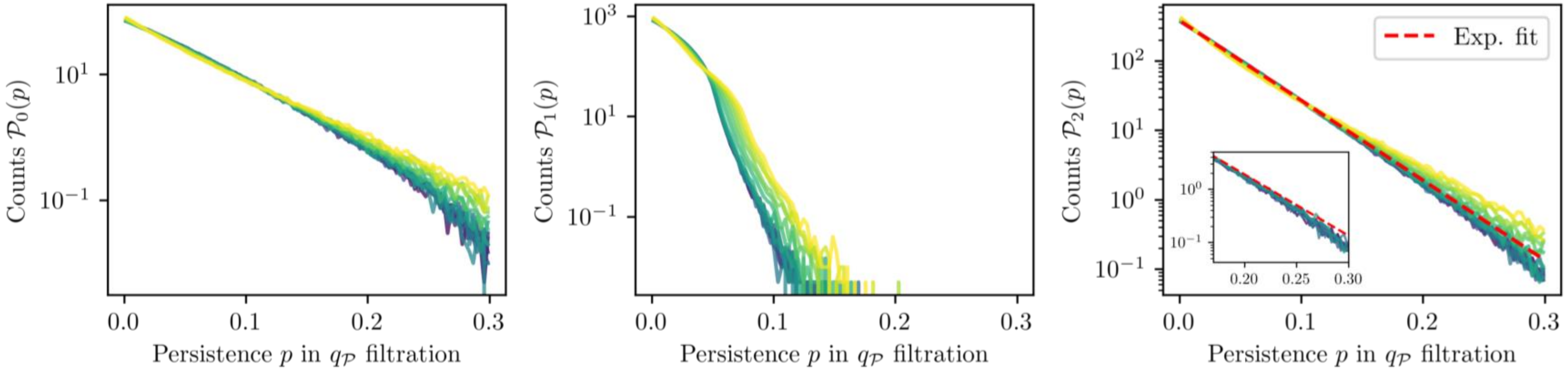

Confinement features from different filtrations

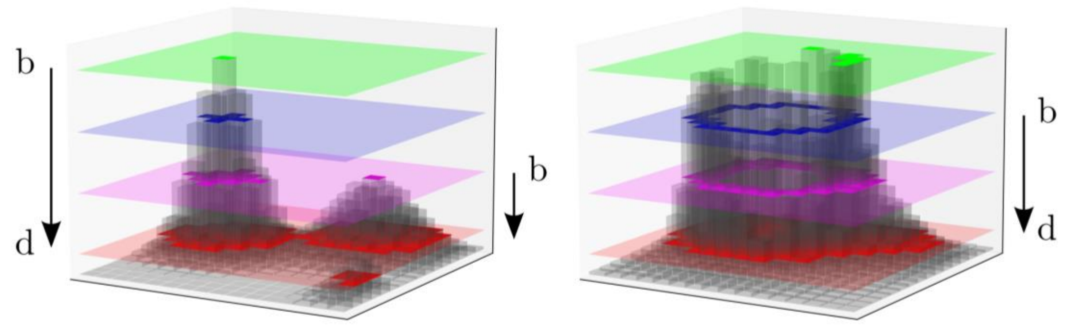

PH of cubical complex superlevel sets, dim. 0 (left), dim. 1 (right).

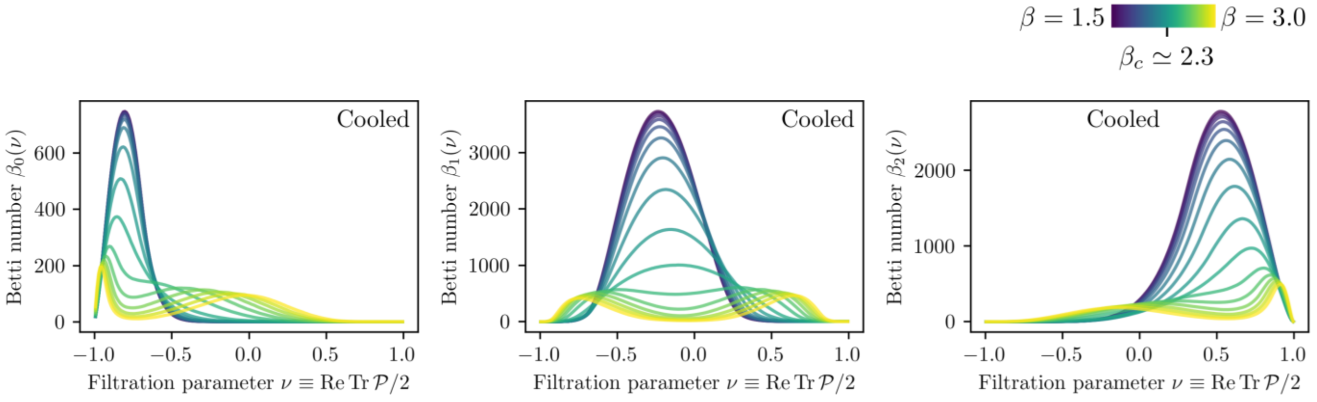

Spontaneously broken center symmetry in Polyakov loop sublevel sets.

Usual topological density $q \sim \mathrm{Tr}\,\mathbf{E} \cdot \mathbf{B}$ often contains strong UV fluctuation signatures. Rewrite top. charge as integral over 3-torus with integrand the Polyakov loop top. density: $q_{\mathcal{P}}(\mathbf{x}) := \frac{1}{24\pi^2}\varepsilon_{ijk}\mathrm{Tr}[(\mathcal{P}^{-1}\partial_i\mathcal{P})(\mathcal{P}^{-1}\partial_j\mathcal{P})(\mathcal{P}^{-1}\partial_k\mathcal{P})]$ [Ford *et al.*, 1998]

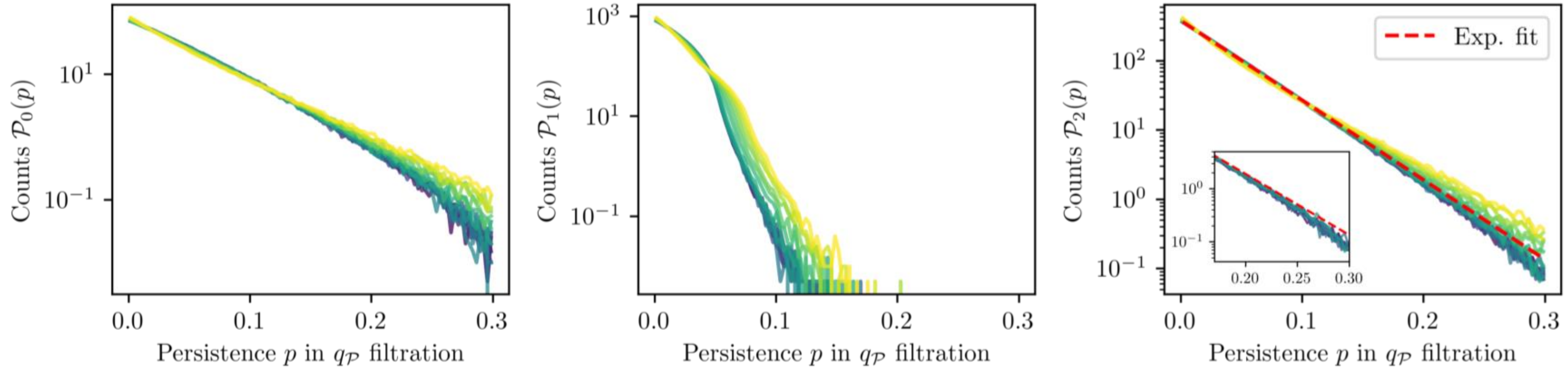

Persistences of Polyakov loop topological density sublevel sets reveal **monopole structures**.

Confinement features from different filtrations

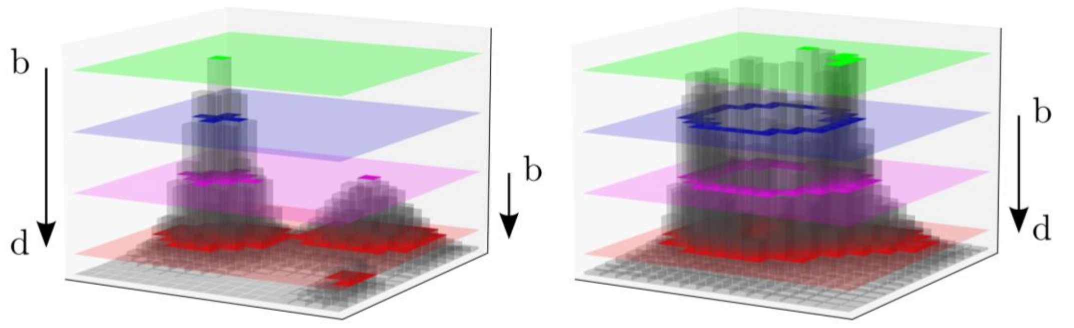

PH of cubical complex superlevel sets, dim. 0 (left), dim. 1 (right).

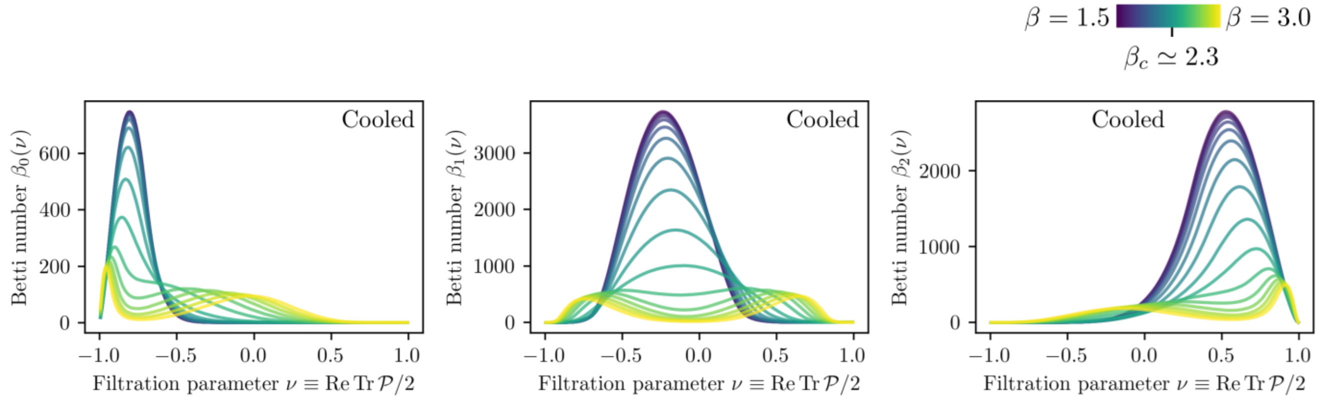

Spontaneously broken center symmetry in Polyakov loop sublevel sets.

Usual topological density $q \sim \mathrm{Tr}\,\mathbf{E}\cdot\mathbf{B}$ often contains strong UV fluctuation signatures. Rewrite top. charge as integral over 3-torus with integrand the Polyakov loop top. density: $q_{\mathcal{P}}(\mathbf{x}) := \frac{1}{24\pi^2}\varepsilon_{ijk}\mathrm{Tr}[(\mathcal{P}^{-1}\partial_i\mathcal{P})(\mathcal{P}^{-1}\partial_j\mathcal{P})(\mathcal{P}^{-1}\partial_k\mathcal{P})]$ [Ford *et al.*, 1998]

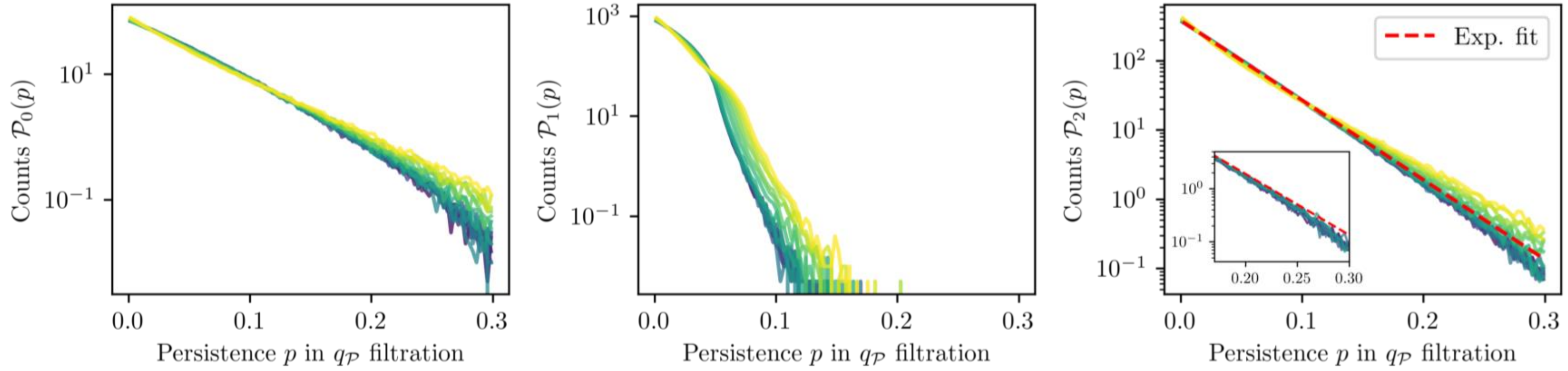

Persistences of Polyakov loop topological density sublevel sets reveal **monopole structures**.

Exponential tails reminiscent of instanton-dyons.

[e.g., Larsen & Shuryak 2016]

Angle-difference filtration of holonomy Lie algebra field

Angle-difference filtration of holonomy Lie algebra field

Polyakov loop in Lie algebra: $\log \mathcal{P}(\mathbf{x}) = i\phi^a(\mathbf{x})T^a$. Trace $P(\mathbf{x}) = \cos\phi(\mathbf{x})$, $\phi(\mathbf{x}) = \sqrt{\phi^a(\mathbf{x})\phi^a(\mathbf{x})}/2$

Angle-difference filtration of holonomy Lie algebra field

Polyakov loop in Lie algebra: $\log \mathcal{P}(\mathbf{x}) = i\phi^a(\mathbf{x})T^a$. Trace $P(\mathbf{x}) = \cos\phi(\mathbf{x})$, $\phi(\mathbf{x}) = \sqrt{\phi^a(\mathbf{x})\phi^a(\mathbf{x})}/2$

Construct angle-difference filtration from differences of $\phi(\mathbf{x})$ between nearest neighbors on lattice, π-periodic (center-symm.). [Sale, Giansiracusa, Lucini 2022]

Angle-difference filtration of holonomy Lie algebra field

Polyakov loop in Lie algebra: $\log \mathcal{P}(\mathbf{x}) = i\phi^a(\mathbf{x})T^a$. Trace $P(\mathbf{x}) = \cos\phi(\mathbf{x})$, $\phi(\mathbf{x}) = \sqrt{\phi^a(\mathbf{x})\phi^a(\mathbf{x})}/2$

Construct angle-difference filtration from differences of $\phi(\mathbf{x})$ between nearest neighbors on lattice, π-periodic (center-symm.). [Sale, Giansiracusa, Lucini 2022]

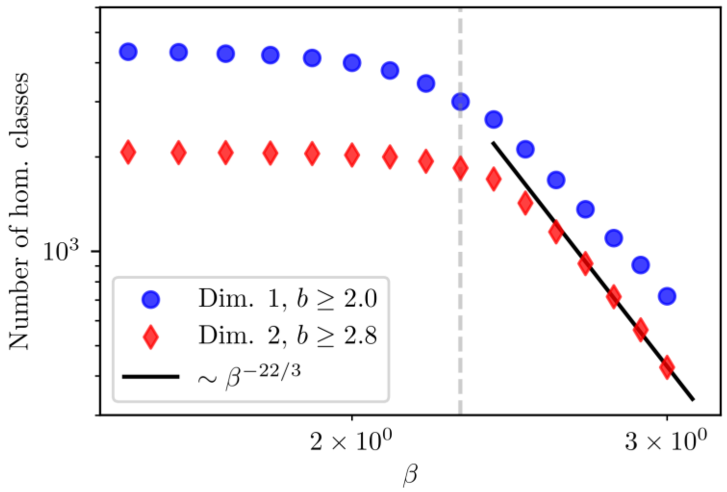

Number homology classes with large birth [DS *et al.*, 2022].

Angle-difference filtration of holonomy Lie algebra field

Polyakov loop in Lie algebra: $\log \mathcal{P}(\mathbf{x}) = i\phi^a(\mathbf{x})T^a$. Trace $P(\mathbf{x}) = \cos\phi(\mathbf{x})$, $\phi(\mathbf{x}) = \sqrt{\phi^a(\mathbf{x})\phi^a(\mathbf{x})}/2$

Construct angle-difference filtration from differences of $\phi(\mathbf{x})$ between nearest neighbors on lattice, π-periodic (center-symm.). [Sale, Giansiracusa, Lucini 2022]

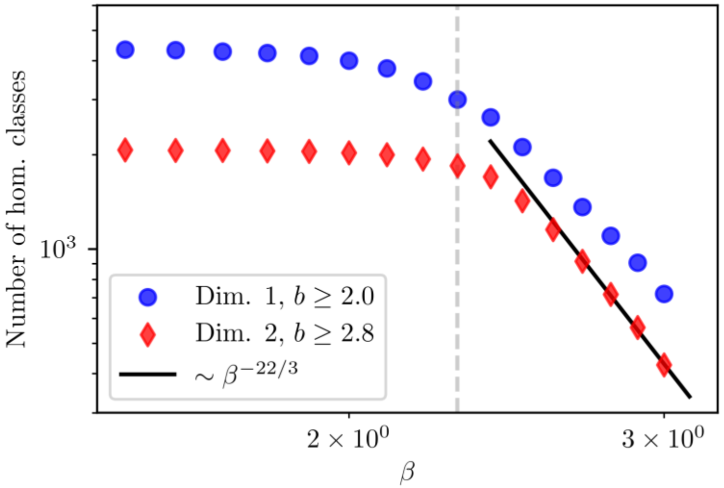

Number homology classes with large birth [DS *et al.*, 2022].

Find in number of lately born homology classes **manifestation of instanton appearance probability**

$$\exp(-S) = \exp(-\frac{8\pi^2}{g^2(T)}) \sim \left(\frac{\Lambda_{\mathrm{UV}}}{T}\right)^b$$

with temperature dependence from one-loop beta function,

$$b = 11N_c/3$$

[e.g., Larsen & Shuryak 2015]

Angle-difference filtration of holonomy Lie algebra field

Polyakov loop in Lie algebra: $\log \mathcal{P}(\mathbf{x}) = i\phi^a(\mathbf{x})T^a$. Trace $P(\mathbf{x}) = \cos\phi(\mathbf{x})$, $\phi(\mathbf{x}) = \sqrt{\phi^a(\mathbf{x})\phi^a(\mathbf{x})}/2$

Construct angle-difference filtration from differences of $\phi(\mathbf{x})$ between nearest neighbors on lattice, π-periodic (center-symm.). [Sale, Giansiracusa, Lucini 2022]

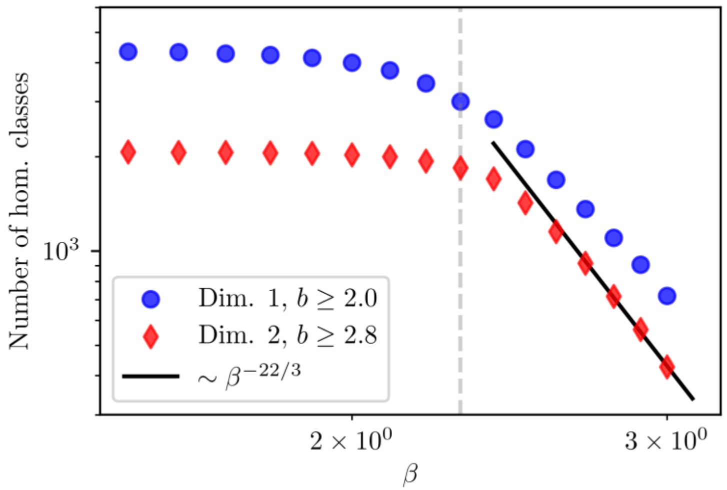

Number homology classes with large birth [DS *et al.*, 2022].

Find in number of lately born homology classes **manifestation of instanton appearance probability**

$$\exp(-S) = \exp(-\frac{8\pi^2}{g^2(T)}) \sim \left(\frac{\Lambda_{\mathrm{UV}}}{T}\right)^b$$

with temperature dependence from one-loop beta function,

$$b = 11N_c/3$$

[e.g., Larsen & Shuryak 2015]

Further filtrations:

Angle-difference filtration of holonomy Lie algebra field

Polyakov loop in Lie algebra: $\log \mathcal{P}(\mathbf{x}) = i\phi^a(\mathbf{x})T^a$. Trace $P(\mathbf{x}) = \cos\phi(\mathbf{x})$, $\phi(\mathbf{x}) = \sqrt{\phi^a(\mathbf{x})\phi^a(\mathbf{x})}/2$

Construct angle-difference filtration from differences of $\phi(\mathbf{x})$ between nearest neighbors on lattice, π-periodic (center-symm.). [Sale, Giansiracusa, Lucini 2022]

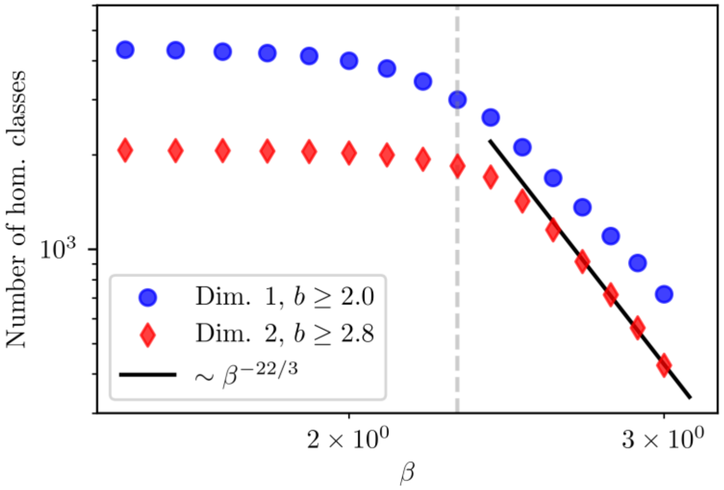

Number homology classes with large birth [DS *et al.*, 2022].

Find in number of lately born homology classes **manifestation of instanton appearance probability**

$$\exp(-S) = \exp(-\frac{8\pi^2}{g^2(T)}) \sim \left(\frac{\Lambda_{\mathrm{UV}}}{T}\right)^b$$

with temperature dependence from one-loop beta function,

$$b = 11N_c/3$$

[e.g., Larsen & Shuryak 2015]

Further filtrations:

- Differences between $\mathrm{Tr}\,\mathbf{E}^2(x)$ and $\mathrm{Tr}\,\mathbf{B}^2(x)$ filtrations due to **electric (Debye) screening outpacing magnetic screening**, both showing clear kink at phase transition.

Angle-difference filtration of holonomy Lie algebra field

Polyakov loop in Lie algebra: $\log \mathcal{P}(\mathbf{x}) = i\phi^a(\mathbf{x})T^a$. Trace $P(\mathbf{x}) = \cos\phi(\mathbf{x})$, $\phi(\mathbf{x}) = \sqrt{\phi^a(\mathbf{x})\phi^a(\mathbf{x})}/2$

Construct angle-difference filtration from differences of $\phi(\mathbf{x})$ between nearest neighbors on lattice, π-periodic (center-symm.). [Sale, Giansiracusa, Lucini 2022]

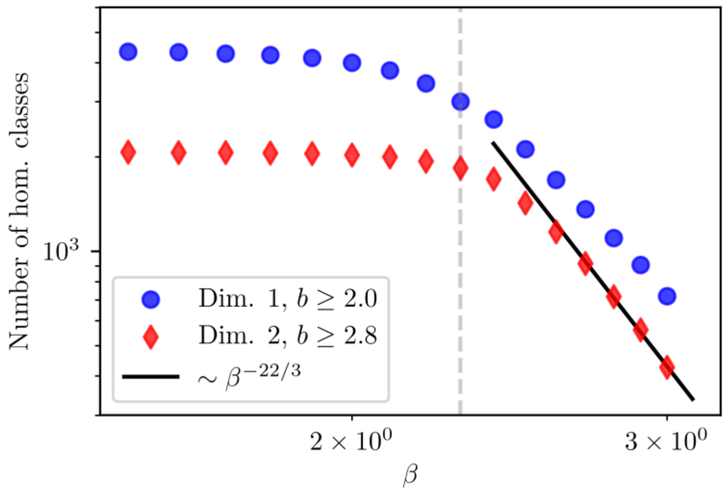

Number homology classes with large birth [DS *et al.*, 2022].

Find in number of lately born homology classes **manifestation of instanton appearance probability**

$$\exp(-S) = \exp\left(-\frac{8\pi^2}{g^2(T)}\right) \sim \left(\frac{\Lambda_{\mathrm{UV}}}{T}\right)^b$$

with temperature dependence from one-loop beta function,

$$b = 11N_c/3$$

[e.g., Larsen & Shuryak 2015]

Further filtrations:

- Differences between $\mathrm{Tr}\,\mathbf{E}^2(x)$ and $\mathrm{Tr}\,\mathbf{B}^2(x)$ filtrations due to **electric (Debye) screening outpacing magnetic screening**, both showing clear kink at phase transition.
- Usual top. density $q \sim \mathrm{Tr}\,\mathbf{E}\cdot\mathbf{B}$ reveals **local lumps** reminiscent of monopoles, too.

Content

1. Lattice improved Hamiltonians for classical-statistical simulations
2. Non-thermal fixed points in persistent homology
3. Confinement in persistent homology
4. Conclusions & outlook

Conclusions

Conclusions

- There are interesting nonequilibrium scenarios still to be explored using classical-statistical simulations, in particular including fermions.

Conclusions

- There are interesting nonequilibrium scenarios still to be explored using classical-statistical simulations, in particular including fermions.
- Persistent homology provides sensitive order parameters for universal and critical phenomena in scalar and gauge theories.

Conclusions

- There are interesting nonequilibrium scenarios still to be explored using classical-statistical simulations, in particular including fermions.
- Persistent homology provides sensitive order parameters for universal and critical phenomena in scalar and gauge theories.
- Self-similarity at nonthermal fixed points is detected by persistent homology; mathematical analyses allow for insights into geometric effects.

Conclusions

- There are interesting nonequilibrium scenarios still to be explored using classical-statistical simulations, in particular including fermions.
- Persistent homology provides sensitive order parameters for universal and critical phenomena in scalar and gauge theories.
- Self-similarity at nonthermal fixed points is detected by persistent homology; mathematical analyses allow for insights into geometric effects.
- Confinement-deconfinement transition can be detected gauge-invariantly via persistent homology observables with interesting characteristics, including links to instantons and dyons.

Outlook

Outlook

- Insights from class.-stat. simulations for quantum information scrambling and chaos via OTOC computation?

Outlook

- Insights from class.-stat. simulations for quantum information scrambling and chaos via OTOC computation?
- With regard to neural network architectures for sampling field configurations: Can topological layers substantially improve these, exploiting the high sensitivity of persistent homology to non-local structures?

Outlook

- Insights from class.-stat. simulations for quantum information scrambling and chaos via OTOC computation?
- With regard to neural network architectures for sampling field configurations: Can topological layers substantially improve these, exploiting the high sensitivity of persistent homology to non-local structures?
- Persistent homology for experimental data, for instance, to learn about the relation to top. defects for thermalization?

Outlook

- Insights from class.-stat. simulations for quantum information scrambling and chaos via OTOC computation?
- With regard to neural network architectures for sampling field configurations: Can topological layers substantially improve these, exploiting the high sensitivity of persistent homology to non-local structures?
- Persistent homology for experimental data, for instance, to learn about the relation to top. defects for thermalization?
- How far can an independent physical interpretation of “homological excitations’’ go?